Research Square

Preprints are preliminary reports that have not undergone peer review.
They should not be considered conclusive, used to inform clinical practice,
or referenced by the media as validated information.

An Enhanced Quantum Image Representation for Improved Intensity Preservation and Fidelity

Vrushali Nikam

vrushali.nikam@ges-coengg.org

MET's BKC IOE,Nashik India

Shirish Sane

GES's R H Sapat COE, Nashik,India

Research Article

Keywords: Quantum Image Representation, IP-QIR, FRQI, NEQR, Intensity Preservation, NISQ Devices

Posted Date: March 3rd, 2026

DOI: https://doi.org/10.21203/rs.3.rs-8893817/v1

License: This work is licensed under a Creative Commons Attribution 4.0 International License.
Read Full License

Additional Declarations: No competing interests reported.

An Enhanced Quantum Image Representation for Improved Intensity Preservation and Fidelity

Vrushali Nikam[1,*]
Department of Computer Engineering
MET's Institute of Engineering, BKC, Adgaon
Nashik, Maharashtra 422003, India
vrushali.nikam@ges-coengg.org

Shirish Sane[2,†]
Department of Computer Engineering
GES's R. H. Sapat College of Engineering, Management Studies and Research
College Road, Nashik, Maharashtra 422005, India
principal@ges-coengg.org

*Corresponding author
†These authors contributed equally to this work.

Abstract: Quantum Image Representation (QIR) is a fundamental concept in quantum image processing. It describes how classical images are converted into quantum states for processing by quantum computers. Researchers have proposed several QIR models, with FRQI and NEQR being the most popular. These models demonstrate the possibilities of quantum image encoding. Nevertheless, they are also limited in some ways. In general, pixel intensity accuracy, the required number of qubits, and circuit complexity have trade-offs. Their application to Noisy Intermediate-Scale Quantum (NISQ) devices is challenging because the quantum resources are small in such devices.
In this paper, we introduce our own approach, the Intensity-Preserving Quantum image representation (IP-QIR). The key aim of IP-QIR is to maintain information about the grayscale intensities and decrease the number of quantum resources. The IP-QIR quantifies the pixel intensities using a controlled rotation scheme. The measurement statistics of a single qubit hold the intensity information, and the position qubits represent the spatial information. The strategy uses small patches of images rather than complete images to facilitate implementation. This will decrease the depth of the circuit design and make the approach less advanced for near-term quantum hardware. IBM Qiskit simulations were used to assess the performance of the IP-QIR. The three types of grayscale images used in the experiments were synthetic image patches, SAR images, and medical TB chest X-ray images. It was revealed that IP-QIR maintains the intensity information compared to FRQI and NEQR. SAR and medical data can reach a fidelity of 84.12%. Another notable point is that the size of a 4×4 image patch only requires five qubits, which is much lower than that in NEQR. Meanwhile, a good reconstruction accuracy was achieved. These findings demonstrate that IP-QIR is an effective and realistic approach to quantum image representation on NISQ-era quantum devices.

Keywords: Quantum Image Representation, IP-QIR, FRQI, NEQR, Intensity Preservation, NISQ Devices

1 Introduction

Quantum computing creates new possibilities in visual information processing. It focuses on new methods for handling and analyzing image data. One important

challenge in this field is the representation of a regular classical image on a quantum computer. Quantum image representation (QIR) methods address this issue by encoding pixel intensity values and their spatial positions into quantum states [1, 2, 3, 4]. This representation empowers image processing and analysis to be performed directly in the quantum domain. QIR is particularly relevant to applications such as medical imaging, remote sensing, and synthetic image analysis. In these areas, accurate preservation of intensity details, reliable image reconstruction, and efficient use of computational resources are crucial. [5, 6, 27, 19].

Over the years, several QIR approaches have proposed by reaserchers. One such method is the flexible representation of quantum images (FRQI). The FRQI encodes pixel positions and grayscale intensity values using amplitude-based rotations. This provides a compact representation and requires a relatively small number of qubits [16, 17]. Another commonly used method is the novel enhanced quantum representation (NEQR). The NEQR represents pixel intensities using basis-state encoding. This allows for an exact intensity representation. However, it requires more qubits and leads to more complex gate structures [9, 10]. Although both FRQI and NEQR demonstrate the potential of quantum-based image encoding, they have certain limitations. In FRQI, the pixel intensities are acquired from probabilistic amplitude measurements. Therefore, small deviations in the intensity values can occur, particularly in the presence of noise [16, 15]. In the case of NEQR, the intensity representation is precise in theory. However, this method requires deeper quantum circuits and a larger number of qubits. This makes its implementation difficult in near-term quantum devices. [6, 15].

Maintaining accurate pixel intensity is especially important in applications such as synthetic aperture radar (SAR) and medical diagnostics. SAR images often contain fine structural and textural details. These details are crucial for correct interpretation and analysis [19, 29, 61]. In medical imaging, such as chest X-rays used for tuberculosis diagnosis, small intensity variations are very important. Even minor changes in intensity can point to important clinical features [5, 27, 62]. Because of this, any reconstruction errors introduced during quantum encoding can reduce the reliability of these images for further analysis [15, 16].

To deal with these problems, we propose a new method called Intensity-Preserving Quantum Image Representation. The main idea is simple as we want to keep pixel intensities accurate but use fewer qubits and simpler circuits. In IP-QIR, intensity values are stored in the measurement probability of a single intensity qubit, while position qubits hold the spatial information. Moreover, the method works on small image patches instead of entire images. This patch-based strategy lowers the number of qubits needed and also reduces the circuit depth. [32, 14].

We tested the IP-QIR using IBM Qiskit simulations on three types of grayscale images. First, we used synthetic image patches with controlled patterns for the baseline evaluation [1, 39]. Next, we used SAR images with high-frequency structures and realistic noise patterns[19, 29, 61]. We then used medical tuberculosis (TB) chest X-ray patches, where small intensity differences are important for accurate diagnosis [5, 40, 62].The results show that IP-QIR retains intensity information better and is more efficient in encoding than FRQI and NEQR. Simultaneously, it uses fewer qubits [15, 40]. Overall, the method provides a good balance between accuracy and resource efficiency [40, 41].

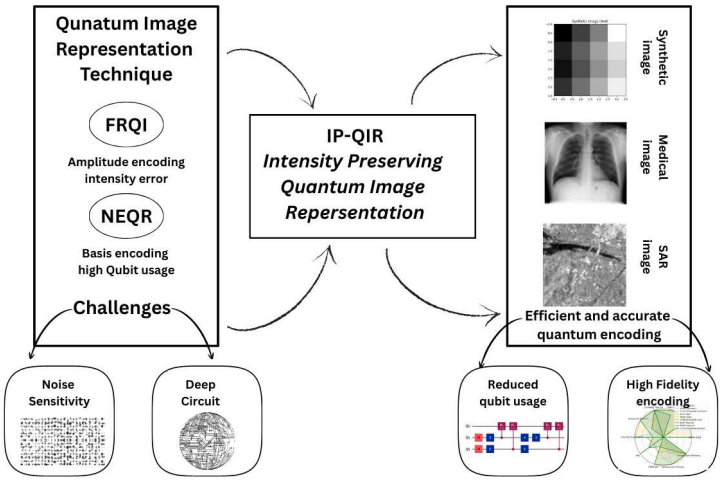


Figure 1: Limitations of FRQI and NEQR and Motivation for the Proposed IP-QIR Representation.

The key contributions of this work are summarized as follows:

1. Introduction of the IP-QIR framework for high-fidelity, intensity-preserving quantum image representation.
2. Comparative evaluation of IP-QIR against FRQI and NEQR across synthetic, SAR, and medical datasets.
3. A patch-based encoding strategy that reduces qubit usage and circuit depth, making it feasible for NISQ devices.
4. Extensive experiments using metrics such as qubit count, circuit depth, encoding efficiency, pixel fidelity, and information preservation.

This paper is organized into the following sections. Section 2 explains the motivation and background of this study. Section 3 presents the problem statement. Section 4 reviews the existing quantum image representation methods and points out the research gap. The proposed IP-QIR approach is described in Section 5. Section 6 introduces the datasets and preprocessing steps. The experimental setup and implementation details are provided in Section 8, with evaluation criteria defined in Section 9. Results and analysis are presented in Section 10, and conclusions and future directions are given in Section 11.

2 Motivation

Quantum image processing is a new area of research in quantum computing. It focuses on how images can be processed using quantum systems. Classical image processing already exists and is effective. However, problems start to appear when images become very large or complex. Scaling is difficult, and parallel processing is limited.

Consequently, quantum image representation methods have been introduced. FRQI [17, 16] and NEQR [9, 10] are two well-known methods for images that attempt to exploit the advantages of quantum computing. However, they still have issues. In many cases, the pixel intensity is not stored perfectly. Some methods require more qubits. Others increase the circuit depth. Therefore, there is always a balance between accuracy, qubits, and circuit complexity [6, 15].

These trade-offs make it difficult to use such methods on Noisy Intermediate-Scale Quantum (NISQ) devices. In these systems, qubits are limited, the circuit depth cannot be very large, and the coherence time is constrained [22, 23]. Therefore, practical deployment is challenging. In applications such as medical imaging and remote sensing, accurate pixel intensity is crucial. Even small intensity differences can sometimes lead to incorrect interpretations of important details [5, 27, 19]. Simultaneously, methods that require too many qubits or very deep circuits are not practical for real NISQ-era quantum devices [15, 16].

The motivation of this work is to design a quantum image representation that preserves pixel intensity with high accuracy and uses quantum resources. This method focuses on patch-based encodings. It also uses simple, controlled rotation gates. Therefore, the limitations of the existing methods are reduced. This makes quantum image processing more suitable for tasks in which accuracy is required [40, 41].

3 Problem Statement

High-resolution image processing is not easy, especially in areas like medical imaging and remote sensing. When quantum image representation methods are used, the problem becomes even harder. Many existing models, such as FRQI and NEQR, work with full-resolution images. Because of that, they need a lot of qubits and very deep circuits. This makes it tough to run them on current quantum simulators or near-term quantum devices.

FRQI represents pixel intensities with a single qubit with rotation angles. This makes image reconstruction probabilistic, and exact intensity values can sometimes be lost. In contrast, NEQR represents pixel values directly in the computational basis, which keeps intensity accurate. However, this requires more qubits and deeper circuits. More approaches, such as MCQI, GQIR, FTQR and QUALPI attempt to trade off qubit and accuracy. Nevertheless, they are not applicable to large datasets, i.e. medical scans or SAR pictures, since they are not scaling.

To address the problems, this work suggests a patch-based Intensity-Preserving Quantum Image Representation. The idea is to split images into smaller patches. This helps lower the number of qubits needed and keeps the circuits simpler. Also, it keeps the intensity of each pixel accurate. In this approach, we can encode and reconstruct synthetic images, SAR images, and medical image patches in a practical way. This makes quantum image processing possible on real datasets without losing fidelity.

The primary objectives of the IP-QIR model are:

1. Intensity Preservation: Ensure that pixel intensity values are accurately represented and reconstructed.
2. Resource Efficiency: Minimize qubit usage and circuit depth, making simulations practical on current quantum platforms.

3. Scalability: Enable processing of real-world image datasets by focusing on smaller patches rather than full images.

The IP-QIR is a solution to the drawbacks of the current methods of quantum image representation. It offers a more viable and effective method of encoding quality images. In this regard, quantum image processing is more appropriate to be used in the real world. This is particularly applicable in fields of medical imaging and remote sensing.

3.1 Research Gap

Even though many quantum image representation (QIR) models have been developed, a clear constraint still exists between intensity accuracy and the use of quantum resources. Probabilistic models such as FRQI [1] are made with fewer qubits, and the circuit is simple to implement. In spite of this, the pixel intensity cannot always be recovered in the reconstruction of the image. This is why FRQI cannot be used in a situation where high accuracy is to be achieved. In contrast, deterministic models like NEQR [4] store pixel intensity values exactly. The problem is that NEQR needs a large number of qubits and very deep quantum circuits. This renders the use of NEQR with large images challenging or even the use of the technique on modern NISQ-era quantum machines.

There are better techniques like MCQI and EFRQI/QRCI [2, 3], which attempt to trade off between image quality and consumptions of quantum resources. Nevertheless, they are not so efficient in terms of encoding large or real-life images. Another issue is that most existing approaches work on the entire image at once. This increases circuit depth and makes practical simulation also implementation on real quantum hardware difficult.

These restrictions underscore the importance of a quantum image representation method which can capture pixel intensity correctly while being quantum resource efficient and be able to scale to large size images. The Intensity Preserving Quantum Image Representation (IP-QIR) is proposed to fulfill this requirement. It is an encoding scheme that relies on patch-based encoding to minimize the number of qubits and maintain a manageable circuit depth, yet is capable of performing high-fidelity intensity reconstruction. This is why it is applicable to real-world data, such as synthetic, SAR, and medical images.

4 Related Work

Quantum Image Representation (QIR) is a mathematical method which provide an encoding of classical image data to quantum states that enables storage, transmission and processing of images with quantum computing methods [1, 2, 3, 4]. In the last 20 years, numerous QIR models have been proposed, primarily varying in their encoding of the position of pixels and intensity values at quantum registers. Each of them also entails some trade-offs, especially on qubit usage, circuit depth, reconstruction accuracy and scalability [5, 6, 7, 1, 9].

Figure 2 illustrates a taxonomy of the principal QIR methods to provide a general picture of the methods and their interconnection. The approaches are classified into three. The former entails spatial-domain methods, in general, representing images in amplitude or basis states, including FRQI [17, 16], NEQR

[9, 5], MCQI [20], GQIR [14]The second types are specialized or advanced techniques which either use frequency-domain, compression, multi-wavelength encoding or structure-sensitive designs such as FTQR [12, 5], QUALPI [13, 3], QRMW [21, 3], EBA-QR/SA-QIR [40, 3]); The third category is an expanded variants which improve the encoding based on amplitude to make it more fidelity. This hierarchical classification emphasizes the way in which the QIR methods have been evolving and the trade-offs that it entails as well as give a clear visual picture of it to the reader before getting to the real discussion(e.g., EFRQI [16, 3], QRCI [15, 3]).

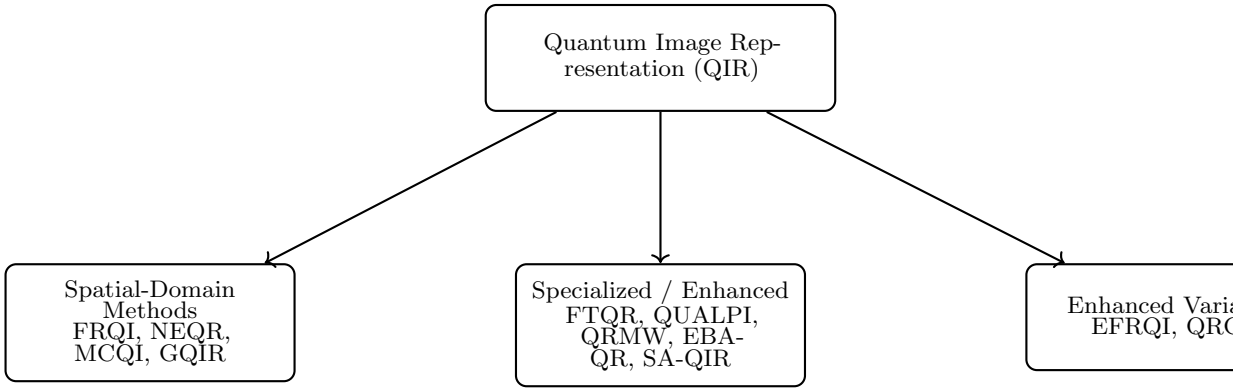


Figure 2: Taxonomy of Quantum Image Representation (QIR) techniques.

4.1 Flexible Representation of Quantum Images (FRQI)

The Flexible Representation of Quantum Images (FRQI) encodes grayscale images by mapping pixel intensity information into the probability amplitudes of a single color qubit, while spatial coordinates are represented using position qubits [17, 16, 15]. The quantum image state is defined as

$$|\Psi_{\text{FRQI}}\rangle = \frac{1}{2^n} \sum_{x=0}^{2^n-1} \sum_{y=0}^{2^n-1} \left(\cos\theta_{x,y}|0\rangle + \sin\theta_{x,y}|1\rangle\right)|x,y\rangle \tag{1}$$

where $\theta_{x,y} \in [0, \pi/2]$ denotes the normalized grayscale intensity of the pixel at position (x, y).

FRQI is highly qubit-efficient and supports relatively shallow quantum circuits, making it attractive for early-stage quantum implementations [16, 15]. However, its probabilistic measurement mechanism causes intensity distortion during image reconstruction, which limits its applicability in domains requiring precise pixel-level fidelity [15, 12].

Consider a simple 2×2 grayscale image with pixel intensities normalized to $[0, 1]$ as follows:

$$\begin{bmatrix} 0.0 & 0.5 \\ 0.75 & 1.0 \end{bmatrix}$$

Using FRQI, the pixel intensity at position (x, y) is encoded into the rotation angle

$$\theta_{x,y} = \arccos(\sqrt{p_{x,y}})$$

where $p_{x,y}$ is the normalized pixel intensity. The corresponding rotation angles are:

$$\theta_{0,0} = \arccos(\sqrt{0.0}) = \frac{\pi}{2}, \quad \theta_{0,1} = \arccos(\sqrt{0.5}) \approx 0.7854$$

$$\theta_{1,0} = \arccos(\sqrt{0.75}) \approx 0.5176, \quad \theta_{1,1} = \arccos(\sqrt{1.0}) = 0$$

The 2×2 FRQI quantum state is then written as:

$$\begin{aligned} |\Psi_{\text{FRQI}}\rangle = \frac{1}{2}((&\cos\theta_{0,0}|0\rangle + \sin\theta_{0,0}|1\rangle)|00\rangle + \\ &(\cos\theta_{0,1}|0\rangle + \sin\theta_{0,1}|1\rangle)|01\rangle + \\ &(\cos\theta_{1,0}|0\rangle + \sin\theta_{1,0}|1\rangle)|10\rangle + \\ &(\cos\theta_{1,1}|0\rangle + \sin\theta_{1,1}|1\rangle)|11\rangle) \end{aligned}$$

Here, the first qubit represents the pixel intensity, while the two position qubits encode the pixel coordinates (x, y). This example demonstrates how FRQI efficiently encodes a small image, though the probabilistic measurement may introduce intensity distortion upon reconstruction [17, 16].

4.2 Novel Enhanced Quantum Representation (NEQR)

The Novel Enhanced Quantum Representation (NEQR) addresses the probabilistic limitation of FRQI by encoding pixel intensity values directly into the computational basis states [9, 1, 7]. The corresponding quantum image state is given by

$$|\Psi_{\text{NEQR}}\rangle = \frac{1}{2^n} \sum_{x=0}^{2^n-1} \sum_{y=0}^{2^n-1} |I_{x,y}\rangle \otimes |x, y\rangle \tag{2}$$

where $|I_{x,y}\rangle$ represents the binary-encoded grayscale intensity of the pixel at position (x, y).

NEQR enables deterministic image reconstruction with exact intensity preservation, making it suitable for accuracy-critical applications [9, 7]. However, this benefit comes at the cost of increased qubit requirements and deeper circuits, significantly limiting its scalability and feasibility on Noisy Intermediate-Scale Quantum (NISQ) devices [2].

Consider a 2×2 grayscale image with pixel intensities (0–3 levels):

$$\begin{bmatrix} 0 & 2 \\ 3 & 1 \end{bmatrix}$$

In NEQR, each pixel intensity is directly encoded into qubits in binary form. Using 2 qubits for intensity and 2 qubits for position, the binary encoding is:

$$0 \to |00\rangle, \quad 1 \to |01\rangle, \quad 2 \to |10\rangle, \quad 3 \to |11\rangle$$

The position qubits are assigned as:

$$(0,0) \to |00\rangle, \quad (0,1) \to |01\rangle, \quad (1,0) \to |10\rangle, \quad (1,1) \to |11\rangle$$

Plugging these into the NEQR formula:

$$\begin{aligned} |\Psi_{\text{NEQR}}\rangle = \frac{1}{2}\Big(& |00\rangle_{\text{intensity}} \otimes |00\rangle_{\text{position}} + |10\rangle_{\text{intensity}} \otimes |01\rangle_{\text{position}} \\ & + |11\rangle_{\text{intensity}} \otimes |10\rangle_{\text{position}} + |01\rangle_{\text{intensity}} \otimes |11\rangle_{\text{position}} \Big) \end{aligned} \tag{3}$$

Here, the first 2 qubits encode pixel intensity in binary. The last 2 qubits encode the pixel coordinates (x, y). NEQR allows exact intensity reconstruction, but requires more qubits and deeper circuits compared to FRQI [2].

4.3 Multi-Channel Quantum Image Representation (MCQI)

The Multi-Channel Quantum Image (MCQI) representation extends FRQI to support color images by encoding RGB intensity components into multiple color qubits [2, 7]. The MCQI quantum state is expressed as

$$\begin{aligned} |\Psi_{\text{MCQI}}\rangle = \frac{1}{2^n} \sum_{x,y} & \left(\cos\theta^R_{x,y}|0\rangle + \sin\theta^R_{x,y}|1\rangle\right) \\ & \left(\cos\theta^G_{x,y}|0\rangle + \sin\theta^G_{x,y}|1\rangle\right) \\ & \left(\cos\theta^B_{x,y}|0\rangle + \sin\theta^B_{x,y}|1\rangle\right)|x,y\rangle \end{aligned} \tag{4}$$

MCQI improves color expressiveness and supports richer visual information. However, the use of multiple color qubits significantly increases circuit depth and quantum resource consumption, which constrains its practical deployment on current quantum hardware [2].

4.4 Generalized Quantum Image Representation (GQIR)

The Generalized Quantum Image Representation (GQIR) supports flexible image dimensions and arbitrary intensity ranges within a unified quantum framework [2]. Unlike fixed-dimension representations, GQIR enables scalable encoding by jointly representing pixel position and intensity information.

The quantum image state in GQIR is formulated as

$$|\Psi_{\text{GQIR}}\rangle = \frac{1}{\sqrt{N}} \sum_{k=0}^{N-1} |P_k\rangle \otimes |I_k\rangle \tag{5}$$

where $|P_k\rangle$ denotes the quantum state corresponding to the pixel position and $|I_k\rangle$ represents the associated pixel intensity.

Although GQIR provides enhanced flexibility compared to earlier QIR models, it is susceptible to phase accumulation and coherence-related errors as image size increases, potentially reducing reconstruction fidelity and limiting robustness on NISQ-era devices [2].

Consider a 2×2 grayscale image with normalized pixel intensities:

$$I = \begin{bmatrix} 0.0 & 0.5 \\ 0.75 & 1.0 \end{bmatrix}$$

Flatten the image in row-major order: $I_0 = 0.0, I_1 = 0.5, I_2 = 0.75, I_3 = 1.0$, and assign position qubits: $|P_0\rangle = |00\rangle$, $|P_1\rangle = |01\rangle$, $|P_2\rangle = |10\rangle$, $|P_3\rangle = |11\rangle$. Using 1 intensity qubit and 2 position qubits, the quantum state is:

$$|\Psi_{\text{GQIR}}\rangle = \frac{1}{2}\Big(|00\rangle \otimes |0.0\rangle + |01\rangle \otimes |0.5\rangle + |10\rangle \otimes |0.75\rangle + |11\rangle \otimes |1.0\rangle\Big)$$

Here, Intensity qubit(s) encode pixel intensity. Position qubits encode spatial coordinates (x, y). GQIR allows flexible image sizes and intensity ranges, but may accumulate phase errors as image dimensions increase.

4.5 Fourier Transform-Based Quantum Representation (FTQR)

The Fourier Transform-Based Quantum Representation (FTQR) encodes image information in the frequency domain by applying the Quantum Fourier Transform (QFT) to a spatial-domain quantum image state [2, 7]. This transformation enables efficient representation of spectral components and supports frequency-domain image analysis.

The FTQR quantum image state is expressed as

$$|\Psi_{\text{FTQR}}\rangle = \text{QFT}\left(|\Psi_{\text{spatial}}\rangle\right) \tag{6}$$

where $|\Psi_{\text{spatial}}\rangle$ represents the quantum state of the image in the spatial domain.

FTQR is particularly effective for spectral filtering and frequency-based processing tasks. However, the transformation results in a loss of direct spatial locality, complicating pixel-wise operations and precise spatial reconstruction, which limits its suitability for applications requiring exact intensity preservation [2, 3].

Consider a 2×2 grayscale image with normalized intensities:

$$I = \begin{bmatrix} 1 & 2 \\ 3 & 4 \end{bmatrix}$$

Flatten the image in row-major order and encode intensities using amplitude encoding:

$$|\Psi_{\text{spatial}}\rangle = \frac{1}{\sqrt{30}}\big(1|00\rangle + 2|01\rangle + 3|10\rangle + 4|11\rangle\big)$$

where the first qubits represent **position** $(|00\rangle, |01\rangle, |10\rangle, |11\rangle)$ and the amplitude encodes intensity. Applying the 2-qubit QFT to the position qubits gives the frequency-domain representation:

$$|\Psi_{\text{FTQR}}\rangle = \frac{1}{\sqrt{30}}\big(1\text{QFT}(|00\rangle) + 2\text{QFT}(|01\rangle) + 3\text{QFT}(|10\rangle) + 4\text{QFT}(|11\rangle)\big)$$

Here, amplitude encodes pixel intensity. QFT operates on position qubits, converting spatial information into frequency components. FTQR enables frequency-domain operations but may reduce spatial reconstruction accuracy relative to purely spatial methods.

4.6 Quantum Image Lossless Processing Interface (QUALPI)

The Quantum Image Lossless Processing Interface (QUALPI) aims to minimize qubit usage by compressing pixel intensity information into compact quantum states, thereby improving storage efficiency in quantum image representations [15, 2]. Spatial information is preserved through position qubits, while intensity values are encoded in a reduced form.

The QUALPI quantum image state can be expressed as

$$|\Psi_{\text{QUALPI}}\rangle = \sum_i \alpha_i |P_i\rangle \otimes |C_i\rangle \tag{7}$$

where $|P_i\rangle$ represents pixel position states and $|C_i\rangle$ denotes compressed intensity information. While QUALPI achieves improved qubit efficiency compared to exact encoding schemes, the compression mechanism can lead to information loss during reconstruction, resulting in reduced intensity fidelity and limiting its applicability in precision-critical imaging tasks [15, 3].

Consider a 2×2 grayscale image with normalized pixel intensities:

$$I = \begin{bmatrix} 0.0 & 0.5 \\ 0.75 & 1.0 \end{bmatrix}$$

Assign position qubits: $|00\rangle, |01\rangle, |10\rangle, |11\rangle$. Using QUALPI, the pixel intensities are compressed into fewer qubits, e.g., mapping each intensity to a 1-qubit compressed state:

$$|C_0\rangle = |0\rangle, \quad |C_1\rangle = |+\rangle, \quad |C_2\rangle = |-\rangle, \quad |C_3\rangle = |1\rangle$$

The quantum state is:

$$|\Psi_{\text{QUALPI}}\rangle = |00\rangle \otimes |0\rangle + |01\rangle \otimes |+\rangle + |10\rangle \otimes |-\rangle + |11\rangle \otimes |1\rangle$$

Here, position qubits encode the spatial coordinates (x, y). Compressed qubits encode intensity in a reduced form to save qubits. QUALPI improves storage and qubit efficiency, but may lose some intensity fidelity during reconstruction [15, 2].

4.7 Quantum Representation of Multi-Wavelength Images (QRMW)

The Quantum Representation of Multi-Wavelength Images (QRMW) extends quantum image encoding to multispectral and multi-wavelength data by jointly representing spatial coordinates, wavelength information, and pixel intensities within a unified quantum state [2, 7, 3]. This representation is particularly suited for applications involving hyperspectral imaging and remote sensing.

The QRMW quantum image state is expressed as

$$|\Psi_{\text{QRMW}}\rangle = \sum_{x,y,\lambda} |I_{x,y,\lambda}\rangle \otimes |x, y\rangle \otimes |\lambda\rangle \tag{8}$$

where $|I_{x,y,\lambda}\rangle$ denotes the intensity value corresponding to spatial position (x, y) and wavelength λ. Although QRMW enables rich spectral analysis and supports advanced imaging modalities, it requires additional quantum registers and controlled operations, leading to increased qubit overhead and circuit depth. These requirements limit its scalability and practical deployment on Noisy Intermediate-Scale Quantum (NISQ) devices [2, 3].

Consider a 2×2 spatial image with 2 wavelengths (λ_0, λ_1) and normalized pixel intensities:

$$I_{\lambda_0} = \begin{bmatrix} 0.0 & 0.5 \\ 0.75 & 1.0 \end{bmatrix}, \quad I_{\lambda_1} = \begin{bmatrix} 1.0 & 0.25 \\ 0.5 & 0.75 \end{bmatrix}$$

Assign position qubits: $|00\rangle, |01\rangle, |10\rangle, |11\rangle$, and wavelength qubits: $|\lambda_0\rangle = |0\rangle, |\lambda_1\rangle = |1\rangle$.

The QRMW quantum state is:

$$\begin{aligned} |\Psi_{\text{QRMW}}\rangle = {} & |0\rangle \otimes |00\rangle \otimes |0\rangle + |0.5\rangle \otimes |01\rangle \otimes |0\rangle \\ & + |0.75\rangle \otimes |10\rangle \otimes |0\rangle + |1.0\rangle \otimes |11\rangle \otimes |0\rangle \\ & + |1.0\rangle \otimes |00\rangle \otimes |1\rangle + |0.25\rangle \otimes |01\rangle \otimes |1\rangle \\ & + |0.5\rangle \otimes |10\rangle \otimes |1\rangle + |0.75\rangle \otimes |11\rangle \otimes |1\rangle \end{aligned}$$

Here, intensity qubits encode pixel intensity for each wavelength. The next two qubits encode spatial coordinates (x, y). The last qubit encodes wavelength. QRMW enables multi-wavelength image representation, but increases qubit count and circuit complexity, which may limit scalability on NISQ devices [2, 3].

4.8 Entropy-Based and Structure-Aware Representations (EBA-QR & SA-QIR)

Entropy-Based Quantum Representation (EBA-QR) and Structure-Aware Quantum Image Representation (SA-QIR) focus on preserving statistical distributions and structural characteristics of images rather than exact pixel-wise intensity values [2, 3, 8]. These approaches aim to capture global image information such as texture, entropy, or structural patterns that are relevant for high-level analysis.

Entropy is commonly used as a quantitative measure and is defined as

$$H = -\sum p_i \log_2 p_i \tag{9}$$

where p_i denotes the probability associated with the i-th pixel or feature component [2]. While such representations are effective for feature-driven tasks, including pattern recognition and structural analysis, they typically introduce additional circuit complexity and do not support precise intensity reconstruction, limiting their applicability in general-purpose and precision-critical quantum imaging applications [3].

Consider a 2×2 grayscale image with normalized pixel intensities:

$$\begin{bmatrix} 0.25 & 0.25 \\ 0.25 & 0.25 \end{bmatrix}$$

In EBA-QR, pixel intensities are treated as probabilities to compute global entropy:

$$p_0 = p_1 = p_2 = p_3 = 0.25$$

The image entropy is calculated as:

$$H = -\sum_{i=0}^{3} p_i \log_2 p_i = -4 \cdot 0.25 \cdot \log_2 0.25 = 2 \text{ bits}$$

In a quantum circuit, this entropy information can guide amplitude encoding or structural feature encoding:

$$|\Psi_{\text{EBA-QR}}\rangle = \sum_{x,y} \sqrt{p_{x,y}}\,|x, y\rangle$$

For our 2×2 example:

$$|\Psi_{\text{EBA-QR}}\rangle = \frac{1}{2}\big(|00\rangle + |01\rangle + |10\rangle + |11\rangle\big)$$

Here, qubits encode global pixel distribution probabilities rather than exact intensities. This representation captures statistical and structural information effectively, but does not preserve exact pixel intensities. It is suitable for pattern recognition, feature extraction, or texture analysis, rather than precision imaging [2, 8].

4.9 Enhanced FRQI Variants (EFRQI)

Enhanced Flexible Representation of Quantum Images (EFRQI) and related variants such as Quantum Representation of Color Images (QRCI) extend the original FRQI framework by introducing refined amplitude encoding strategies to improve the expressiveness of pixel intensity representation while maintaining low qubit requirements [2, 3].

$$|\Psi_{\text{EFRQI}}\rangle = \sum_{x,y} \left(\alpha_{x,y}|0\rangle + \beta_{x,y}|1\rangle\right)|x, y\rangle \tag{10}$$

In this formulation, $\alpha_{x,y}$ and $\beta_{x,y}$ are functions of the normalized pixel intensity at position (x, y). These variants aim to reduce intensity distortion and enhance visual quality compared to FRQI [2]. However, since intensity information remains encoded in probability amplitudes, the reconstruction process is still probabilistic, resulting in residual intensity degradation and limiting their suitability for precision-critical imaging applications [3].

Consider a 2×2 grayscale image with normalized pixel intensities:

$$\begin{bmatrix} 0.0 & 0.5 \\ 0.75 & 1.0 \end{bmatrix}$$

The amplitude coefficients are computed as:

$$\alpha_{x,y} = \cos\left(\frac{\pi}{2} p_{x,y}\right), \quad \beta_{x,y} = \sin\left(\frac{\pi}{2} p_{x,y}\right)$$

Thus, for each pixel:

$$
\begin{aligned}
&(0,0) : \alpha_{0,0} = 1, \quad \beta_{0,0} = 0 \\
&(0,1) : \alpha_{0,1} \approx 0.707, \quad \beta_{0,1} \approx 0.707 \\
&(1,0) : \alpha_{1,0} \approx 0.383, \quad \beta_{1,0} \approx 0.924 \\
&(1,1) : \alpha_{1,1} = 0, \quad \beta_{1,1} = 1
\end{aligned}
$$

The 2×2 EFRQI quantum state is then:

$$
\begin{aligned}
|\Psi_{\text{EFRQI}}\rangle = \alpha_{0,0}|0\rangle \otimes |00\rangle + \alpha_{0,1}|0\rangle \otimes |01\rangle \\
+ \alpha_{1,0}|0\rangle \otimes |10\rangle + \alpha_{1,1}|0\rangle \otimes |11\rangle \\
+ \beta_{0,0}|1\rangle \otimes |00\rangle + \beta_{0,1}|1\rangle \otimes |01\rangle \\
+ \beta_{1,0}|1\rangle \otimes |10\rangle + \beta_{1,1}|1\rangle \otimes |11\rangle
\end{aligned}
$$

Here, the first qubit encodes pixel intensity probabilistically using amplitudes $(\alpha_{x,y}, \beta_{x,y})$. The last 2 qubits encode pixel coordinates (x, y). EFRQI reduces intensity distortion compared to FRQI but remains probabilistic, with potential residual reconstruction errors [2, 3].

5 Proposed Method: Intensity Preserving Quantum Image Representation (IP-QIR)

This section introduces the proposed Intensity-Preserving Quantum Image Representation (IP-QIR), a quantum image encoding framework designed to overcome the limitations of existing quantum image representation techniques, namely probabilistic intensity reconstruction, excessive qubit consumption, and high circuit depth. The primary objective of IP-QIR is to achieve accurate preservation of pixel intensity information while maintaining resource efficiency, thereby enabling practical implementation on Noisy Intermediate-Scale Quantum (NISQ) devices.

Unlike conventional amplitude-based or basis-state encoding schemes, IP-QIR adopts a hybrid intensity mapping strategy that preserves grayscale information through controlled amplitude assignment, while requiring fewer qubits and moderate circuit complexity. This design makes IP-QIR suitable for real-world image datasets, including synthetic, SAR, and medical images.

5.1 IP-QIR Framework Overview

The IP-QIR framework encodes grayscale image information into a quantum state by jointly representing pixel position and intensity through controlled quantum operations. The complete encoding workflow consists of the following stages:

1. Image Preprocessing: Input images are resized to dimensions of $2^n \times 2^n$ to match quantum register requirements. Pixel intensities are normalized to the range $[0, 1]$ to facilitate amplitude-based encoding.

2. Intensity Mapping: Each normalized pixel intensity is mapped to a rotation angle that determines the probability amplitudes of the intensity qubit.

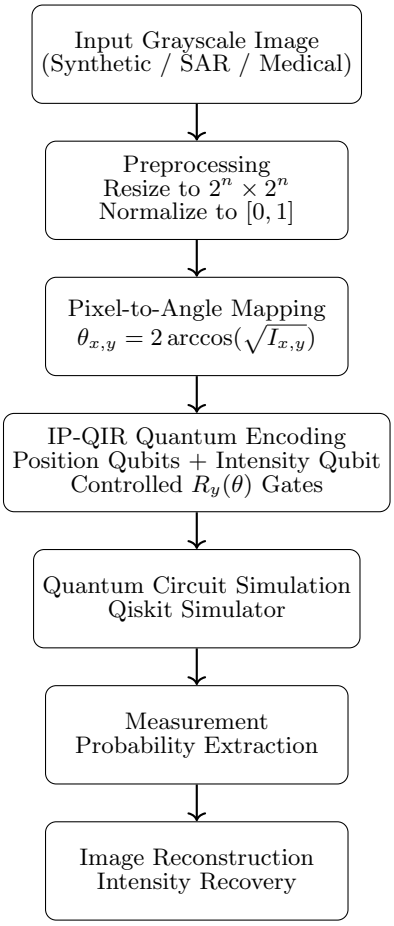


Figure 3: Workflow of the proposed IP-QIR framework

3. Quantum Circuit Construction: A quantum circuit is constructed using position qubits and a single intensity qubit, where multi-controlled rotation gates encode pixel intensities conditioned on spatial coordinates.

4. Quantum Simulation and Measurement: The constructed circuit is simulated using the IBM Qiskit quantum simulator, and measurement statistics are obtained.

5. Image Reconstruction and Evaluation: The original image is reconstructed from measurement outcomes, and performance metrics such as fidelity, information loss, and circuit complexity are computed.

The overall workflow of the proposed IP-QIR framework is illustrated in Fig. 3.

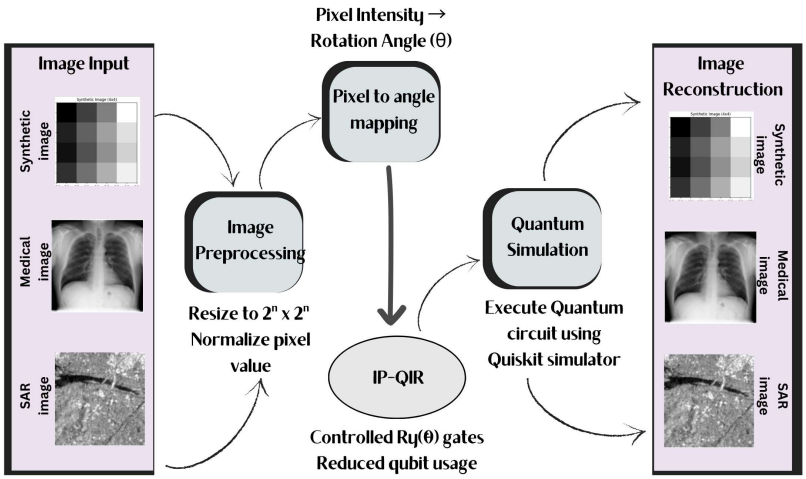


Figure 4: Architecture of the proposed IP-QIR system, showing preprocessing, quantum encoding, simulation, and image reconstruction stages.

5.2 System Architecture

The proposed Intensity-Preserving Quantum Image Representation (IP-QIR) follows a structured workflow from classical image input to quantum-based reconstruction. It begins with a grayscale image from synthetic, SAR, or medical datasets. During preprocessing, the image is resized to $2^n \times 2^n$ and pixel values are normalized to $[0, 1]$ for compatibility with quantum encoding.

Pixel intensities are then converted to rotation angles using pixel-to-angle mapping, linking classical values to quantum gate parameters. Quantum encoding is applied with position qubits and a single intensity qubit, where controlled $R_y(\theta)$ rotations efficiently encode each pixel's brightness, minimizing qubit usage while keeping circuit depth manageable.

The quantum circuit is simulated using IBM Qiskit, and measurements extract probability distributions. These probabilities are then used to reconstruct the classical image, accurately recovering pixel intensities.

This architecture provides an efficient and practical approach for quantum image representation, balancing accuracy with resource requirements. The workflow is illustrated in Fig. 3.

5.3 Mathematical Formulation of IP-QIR

Let I denote a grayscale image of size $M \times N$, where each pixel intensity $I_{x,y} \in [0, 1]$ represents the normalized grayscale value at spatial position (x, y). The corresponding Intensity-Preserving Quantum Image Representation (IP-QIR) quantum state is defined as:

$$|\Psi_{\text{IP-QIR}}\rangle = \sum_{x=0}^{M-1} \sum_{y=0}^{N-1} \left(\sqrt{I_{x,y}} \, |x, y\rangle|0\rangle + \sqrt{1 - I_{x,y}} \, |x, y\rangle|1\rangle \right) \tag{11}$$

where:

- $|x, y\rangle$ denotes the quantum basis state encoding the pixel position. Specifically, $\lceil \log_2 M \rceil$ qubits represent the x-coordinate and $\lceil \log_2 N \rceil$ qubits represent the y-coordinate.
- $|0\rangle$ and $|1\rangle$ correspond to the computational basis states of the intensity qubit.
- $\sqrt{I_{x,y}}$ and $\sqrt{1 - I_{x,y}}$ are the probability amplitudes of measuring the intensity qubit in $|0\rangle$ and $|1\rangle$, respectively, ensuring that

  $$\Pr(|0\rangle) = |\sqrt{I_{x,y}}|^2 = I_{x,y}, \quad \Pr(|1\rangle) = |\sqrt{1 - I_{x,y}}|^2 = 1 - I_{x,y}.$$

  This guarantees that the measured intensity reflects the original pixel value.
- The summation over all x and y positions creates a superposition encoding the entire image simultaneously, enabling parallel processing.

This amplitude-based encoding ensures improved intensity preservation compared to probabilistic rotation-based methods like FRQI, while requiring only one intensity qubit per pixel (or patch). The approach is particularly suitable for small image patches, allowing shallow quantum circuits and efficient simulation on NISQ-era devices.

5.3.1 Example of IP-QIR (2×2 Image)

Consider a 2×2 grayscale image with normalized pixel intensities:

$$I = \begin{bmatrix} 0.0 & 0.5 \\ 0.75 & 1.0 \end{bmatrix}$$

Using the IP-QIR framework, each pixel at position (x, y) is encoded into the quantum state as an amplitude of the intensity qubit. The corresponding quantum state is defined as:

$$|\Psi_{x,y}\rangle = \sqrt{I_{x,y}} \, |x, y\rangle|0\rangle + \sqrt{1 - I_{x,y}} \, |x, y\rangle|1\rangle$$

In the quantum circuit, this amplitude encoding is realized using a controlled R_y rotation on the intensity qubit, with the rotation angle given by:

$$\theta_{x,y} = 2 \arccos\left(\sqrt{I_{x,y}}\right)$$

Compute the amplitudes and corresponding rotation angles for each pixel:

$$
\begin{aligned}
&(0,0): \quad \sqrt{I_{0,0}} = 0, \quad \sqrt{1-I_{0,0}} = 1, \quad \theta_{0,0} = 2\arccos(0) = \pi \\
&(0,1): \quad \sqrt{I_{0,1}} \approx 0.707, \quad \sqrt{1-I_{0,1}} \approx 0.707, \quad \theta_{0,1} = 2\arccos(0.707) \approx \frac{\pi}{2} \\
&(1,0): \quad \sqrt{I_{1,0}} \approx 0.866, \quad \sqrt{1-I_{1,0}} \approx 0.5, \quad \theta_{1,0} = 2\arccos(0.866) \approx 0.5236 \\
&(1,1): \quad \sqrt{I_{1,1}} = 1, \quad \sqrt{1-I_{1,1}} = 0, \quad \theta_{1,1} = 2\arccos(1) = 0
\end{aligned}
$$

Assign position qubits for spatial encoding:

$$
|00\rangle \to (0,0), \quad |01\rangle \to (0,1), \quad |10\rangle \to (1,0), \quad |11\rangle \to (1,1)
$$

The complete 2×2 IP-QIR quantum state can then be written as:

$$
\begin{aligned}
|\Psi_{\text{IP-QIR}}\rangle = &0 \cdot |00\rangle|0\rangle + 1 \cdot |00\rangle|1\rangle + \\
&0.707 \cdot |01\rangle|0\rangle + 0.707 \cdot |01\rangle|1\rangle + \\
&0.866 \cdot |10\rangle|0\rangle + 0.5 \cdot |10\rangle|1\rangle + \\
&1 \cdot |11\rangle|0\rangle + 0 \cdot |11\rangle|1\rangle
\end{aligned}
$$

Here:

- The first qubit encodes pixel intensity probabilistically. Measuring it yields:

$$
\Pr(|0\rangle) = I_{x,y}, \quad \Pr(|1\rangle) = 1 - I_{x,y}
$$

- The last two qubits encode the spatial coordinates (x, y).
- The controlled $R_y(\theta)$ gate in the quantum circuit implements these amplitudes, ensuring that the probability of measuring $|0\rangle$ for each pixel matches the original intensity.

This example demonstrates that IP-QIR faithfully preserves pixel intensities while requiring only one intensity qubit per pixel, resulting in a compact and efficient quantum encoding suitable for NISQ devices.

5.4 Quantum Circuit Design

The proposed Intensity-Preserving Quantum Image Representation (IP-QIR) encodes grayscale image information using a compact and logically structured quantum circuit composed of position and intensity qubits.

- Position Qubits: A total of $n_x + n_y$ qubits are used to encode the spatial coordinates (x, y) of each pixel, where $n_x = \log_2 M$ and $n_y = \log_2 N$ for an image of size $M \times N$. These qubits uniquely identify the pixel location within the image grid.
- Intensity Qubit: A single qubit is dedicated to encoding the grayscale intensity of each pixel. Pixel values are normalized to the range $[0, 1]$ prior to encoding.

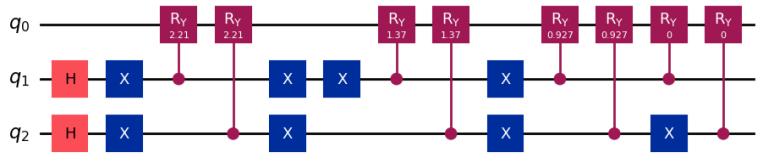


Figure 5: Conceptual 2×2 IP-QIR quantum circuit. Two position qubits encode spatial information, while a single intensity qubit stores grayscale values through controlled $R_y(\theta_{x,y})$ rotations.

– Controlled Rotation Encoding: Pixel intensities are mapped to the intensity qubit using multi-controlled rotation gates. For each pixel at position (x, y), a controlled $R_y(\theta_{x,y})$ gate is applied, where the rotation angle is defined as

$$\theta_{x,y} = 2 \arccos\left(\sqrt{I_{x,y}}\right).$$

This formulation ensures that the probability of measuring the intensity qubit in the $|0\rangle$ state corresponds directly to the original normalized pixel intensity $I_{x,y}$.

– Conditional Association: Each $R_y(\theta_{x,y})$ operation is conditionally applied based on the corresponding position qubit states, guaranteeing a correct association between pixel location and intensity value.

Figure 5 illustrates the conceptual IP-QIR quantum circuit for a 2×2 image, where two position qubits control the rotation applied to a single intensity qubit. This circuit representation reflects the logical encoding mechanism of the proposed method and forms the basis for scalable IP-QIR implementations.

5.5 Algorithmic Workflow

Intensity-Preserving Quantum Image Representation (IP-QIR) is a systematic process review that encodes grayscale images into the quantum system with high precision in maintaining intensity as well as utilising the quantum resources efficiently. The preprocessing stage in the workflow is an activity that receives the input image and resizes it to $2^n \times 2^n$ and normalises the pixel intensity values to $[0, 1]$. Position qubits encode existing spatial information, and there is a special intensity qubit which records the intensity of each pixel. To calculate the rotation angle of each pixel, the normalized intensity is used to compute the rotation angle, and the qubits of position are entangled with the qubits of intensity using a multi-controlled R_y gate. At last, quantum measurements are carried out, and the image is reconstrued with probabilistic results to measure quantum measurements, e.g., fidelity and preservation of intensity. The encoding process is intuitively obvious as it is depicted in Figure 6 where position and intensity qubits interact. This workflow is optimally balanced between the depth of the circuit, the efficiency of the qubits, and the accuracy of the representation, and thus IP-QIR will allow the use of NISQ pieces of equipment.

Algorithm 1 IP-QIR Quantum Image Encoding Algorithm

Require: Grayscale image I of size $M \times N$
Ensure: Quantum image state $|\Psi_{\text{IP-QIR}}\rangle$
1: Resize I to $2^n \times 2^n$
2: Normalize pixel intensities to $[0, 1]$
3: Initialize quantum registers:
    Position qubits
    Intensity qubit
4: **for** each pixel (x, y) in the resized image **do**
5: $\theta_{x,y} \leftarrow 2 \arccos\left(\sqrt{I_{x,y}}\right)$
6: Apply multi-controlled $R_y(\theta_{x,y})$ gate on the intensity qubit controlled by position qubits (x, y)
7: **end for**
8: Measure all qubits
9: Reconstruct image from measurement probabilities
10: Compute performance metrics:
    Fidelity
    Intensity preservation
11: **return** $|\Psi_{\text{IP-QIR}}\rangle$

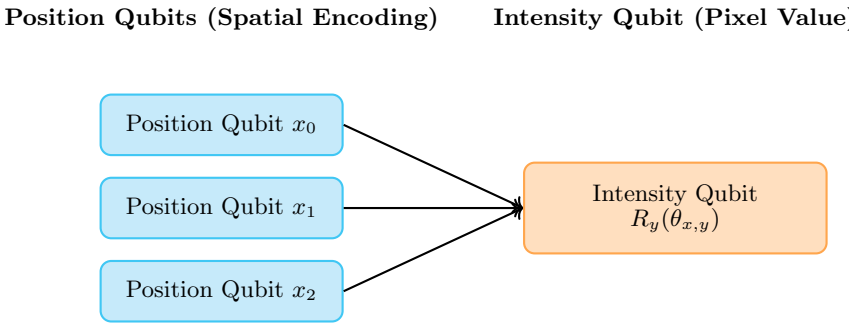


Figure 6: Schematic representation of IP-QIR pixel encoding. Position qubits control the rotation of a single intensity qubit to encode grayscale values efficiently.

5.6 Key Characteristics

The proposed IP-QIR framework exhibits the following key properties:

- Enhanced pixel intensity preservation through controlled amplitude encoding.
- Reduced qubit requirements compared to computational basis encoding schemes.
- Moderate circuit depth compatible with NISQ-era quantum hardware.
- Scalability across synthetic, SAR, and medical image datasets.
- Seamless integration with quantum simulation platforms such as IBM Qiskit.

5.7 Evaluation Criteria

The effectiveness of the proposed IP-QIR representation is assessed using the following criteria:

- Intensity Fidelity: Agreement between original and reconstructed pixel intensities.
- Encoding Time: Time required to construct and simulate the quantum circuit.
- Circuit Complexity: Number of qubits and quantum gates used in the encoding process.
- Scalability: Consistency of performance across different image sizes and datasets.

6 Dataset Description

In order to determine the effectiveness and generalizability of the proposed Intensity-Preserving Quantum Image Representation (IP-QIR), experiments are performed on three types of dataset including synthetic images, Synthetic Aperture Radar (SAR) images, and medical tuberculosis (TB) chest X-ray images. These datasets are chosen to check the strength of the proposed approach in the cases of controlled, real-world, and medically critical imaging.

6.1 Synthetic Images

Synthetic images are artificially generated grayscale images used to validate the fundamental behavior of quantum image encoding techniques. Due to their simplicity and controlled intensity patterns, they enable precise analysis of intensity preservation and circuit complexity.

- Image Size: 2×2 and 4×4 pixels.
- Intensity Range: Pixel values normalized to $[0, 1]$.
- Purpose: To verify the correctness of the IP-QIR encoding process, analyze qubit requirements, circuit depth, and measure pixel-wise fidelity.

6.2 Synthetic Aperture Radar (SAR) Images

SAR images are widely used in remote sensing applications and contain complex structural and textural information represented in grayscale form. These images are suitable for evaluating the ability of IP-QIR to preserve high-frequency spatial details [61].

- Source: Publicly available on Kaggle SAR image datasets [61].
- Image Size: 4×4 pixel patches extracted from larger SAR images.
- Characteristics: Rich structural patterns with varying intensity distributions.
- Purpose: To assess the performance of IP-QIR in preserving spatial patterns and minimizing information loss in real-world imaging data.

6.3 Medical TB Chest X-ray Images

Medical imaging data, specifically TB chest X-ray images, are used to examine the applicability of IP-QIR in healthcare-related scenarios. In medical diagnosis, accurate intensity preservation is crucial, as subtle intensity variations may correspond to pathological changes [62].

- Source: Publicly available on Kaggle TB chest X-ray datasets [62].
- Image Size: 4×4 pixel patches for feasibility of quantum simulation.
- Characteristics: Contains diverse intensity patterns corresponding to anatomical structures and abnormalities.
- Purpose: To demonstrate the robustness of IP-QIR in preserving fine-grained intensity information required for reliable medical image reconstruction.

6.4 Preprocessing

Prior to quantum encoding, all datasets undergo a common preprocessing pipeline to ensure compatibility with quantum image representation:

1. Resizing: Images are resized to $2^n \times 2^n$ dimensions to match the requirements of quantum position encoding.
2. Normalization: Pixel intensities are scaled to the range $[0, 1]$ for amplitude-based quantum encoding.
3. Patch Extraction: For SAR and medical datasets, small image patches are extracted to reduce circuit complexity and enable efficient simulation.

These datasets collectively enable a comprehensive evaluation of the proposed IP-QIR framework in terms of **intensity preservation, circuit efficiency, and reconstruction fidelity** across diverse imaging domains.

7 Image Representation in Quantum State

The aim of quantum image representation is to encode classical image data to the quantum state, and provide parallelism and promising benefits in data compression, security and computational efficiency. The proposed Intensity-Preserving Quantum Image Representation (IP-QIR) is a prototype representing in this work to optimally retain the pixel intensity data with minimum qubit utilization and circuit volume.

7.1 Quantum Representation of Images

In IP-QIR, a grayscale image of size $2^n \times 2^n$ is represented as a composite quantum state consisting of position qubits and intensity qubits. The position qubits encode the spatial coordinates of each pixel, while the intensity qubits store the corresponding grayscale information.

The quantum state representation of an image I can be expressed as:

$$|I\rangle = \sum_{i=0}^{N-1} \alpha_i |p_i\rangle |c_i\rangle \tag{12}$$

where:

- $N = 2^{2n}$ denotes the total number of pixels in the image,
- $|p_i\rangle$ represents the quantum state encoding the position of the i-th pixel,
- $|c_i\rangle$ denotes the quantum state encoding the intensity information,
- α_i is the normalized amplitude associated with the pixel intensity.

This formulation allows the entire image to be stored in a single quantum superposition state, enabling efficient quantum processing.

7.2 IP-QIR Encoding Strategy

The IP-QIR framework introduces an enhanced encoding strategy to improve intensity preservation compared to conventional approaches such as FRQI and NEQR. The encoding process consists of the following steps:

1. Position Encoding: Pixel coordinates are mapped to computational basis states using position qubits corresponding to row and column indices.
2. Intensity Encoding: Pixel intensities are encoded using amplitude-preserving rotations, ensuring accurate mapping of grayscale values into quantum states.
3. Circuit Optimization: Controlled rotation and phase gates are employed to efficiently encode intensity information while reducing circuit depth and gate count.

This encoding strategy enables IP-QIR to achieve higher fidelity while maintaining scalability and efficiency.

7.3 Illustrative Example: 2×2 Image

For a 2×2 grayscale image patch, two position qubits are sufficient to encode all pixel locations:

$$|00\rangle \rightarrow \text{Top-left pixel}$$
$$|01\rangle \rightarrow \text{Top-right pixel}$$
$$|10\rangle \rightarrow \text{Bottom-left pixel}$$
$$|11\rangle \rightarrow \text{Bottom-right pixel}$$

An additional qubit is used to encode pixel intensity information through controlled rotation operations. This representation enables accurate reconstruction of the original image with minimal information loss.

7.4 Advantages of IP-QIR Representation

Compared to existing quantum image representation techniques, IP-QIR offers several advantages:

- High Intensity Fidelity: Accurate preservation of pixel intensity values leads to improved reconstruction quality.
- Reduced Qubit Requirements: Fewer qubits are required compared to NEQR, particularly for larger images.
- Optimized Circuit Depth: Reduced gate count and circuit depth improve feasibility on NISQ devices and enhance robustness against noise.

The proposed quantum image representation forms the foundation for subsequent quantum image operations, measurement, and reconstruction, enabling a comprehensive comparison with FRQI, NEQR, and other existing quantum image encoding schemes.

8 Experimental Setup

This section describes the experimental configuration and procedures used to evaluate the proposed Intensity-Preserving Quantum Image Representation (IP-QIR). The experiments aim to demonstrate the effectiveness of IP-QIR in preserving pixel intensity while optimizing quantum resource utilization and computational efficiency. Evaluations were performed on synthetic images, SAR urban imagery, and medical TB chest X-ray patches using IBM Qiskit quantum simulators under NISQ-inspired constraints.

8.1 Datasets

To ensure comprehensive validation, three datasets with distinct characteristics were employed:

- Synthetic Images: Grayscale images of sizes 2×2 and 4×4 were generated to verify the correctness of the quantum encoding algorithm. These images provide controlled pixel intensities, facilitating precise evaluation of reconstruction fidelity and circuit behavior.
- SAR Urban Imagery: Grayscale patches extracted from SAR images were utilized to assess the robustness of IP-QIR on real-world data with high contrast, structural complexity, and inherent noise.
- Medical TB Chest X-ray Images: Cropped grayscale patches from publicly available TB chest X-ray datasets were employed to evaluate the capability of IP-QIR to preserve subtle intensity variations critical for medical diagnosis.

8.2 Hardware and Software Environment

All experiments were conducted on classical quantum simulators with the following configuration:

- Processor: Intel Core i5 (10th Generation), 2.6 GHz
- Memory: 16 GB RAM
- Operating System: Windows 11
- Software Stack: Python 3.11, IBM Qiskit 0.47.1, NumPy, OpenCV, and Matplotlib

Quantum circuits were simulated using the Qiskit Aer simulator. While no physical quantum hardware was used, all designs adhered to NISQ-era constraints, such as limited qubit counts and shallow circuit depth.

8.3 Quantum Circuit Implementation

The experimental evaluation included a comparison between existing quantum image representations and the proposed IP-QIR:

- FRQI and NEQR: Standard implementations of FRQI and NEQR were developed according to their original formulations and served as baseline methods.
- IP-QIR: Proposed circuits use minimal position and intensity qubits. Controlled R_y rotation gates and multi-controlled operations encode pixel intensities, while SWAP gates are applied for position manipulation where necessary.
- Circuit Metrics: Qubit count, gate count, and circuit depth were recorded for each method and dataset to quantify computational efficiency and resource utilization.

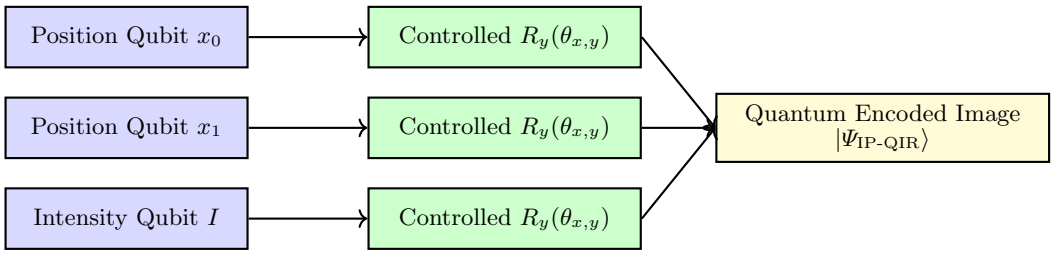


Figure 7: Simplified IP-QIR quantum circuit showing controlled rotations on position and intensity qubits converging to a single quantum encoded image state.

8.4 Experimental Procedure

The experimental workflow consisted of the following steps:

1. Preprocessing: Resize images to $2^n \times 2^n$ dimensions and normalize pixel intensities to $[0, 1]$.
2. Quantum Encoding: Encode images using FRQI, NEQR, and IP-QIR circuits.
3. Simulation: Execute quantum circuits on the Qiskit Aer simulator, performing multiple runs to account for probabilistic outcomes.
4. Measurement and Reconstruction: Extract measurement probabilities to reconstruct classical images.
5. Comparative Analysis: Evaluate pixel fidelity, information loss, qubit usage, circuit depth, and encoding time for all methods.

9 Performance Parameters

The performance of the proposed Intensity-Preserving Quantum Image Representation (IP-QIR) is quantitatively evaluated using multiple metrics that capture quantum resource utilization, computational efficiency, and image reconstruction fidelity. Comparative analysis is performed against two widely adopted quantum image representation models, FRQI [17] and NEQR [9], across three representative datasets: synthetic grayscale images, synthetic aperture radar (SAR) urban patches [61], and medical tuberculosis (TB) chest X-ray images [62].

The evaluation considers both quantum hardware constraints and image quality metrics, providing a holistic assessment of the method's practical applicability, particularly on Noisy Intermediate-Scale Quantum (NISQ) devices [22, 23, 1, 3].

9.1 Number of Qubits

The total number of qubits Q required to encode an image of size $N \times N$ with C-bit intensity representation is a critical factor that directly impacts the scalability of quantum image processing [17, 9, 1]:

$$Q_{\text{NEQR}} = \log_2(N^2)+C, \quad Q_{\text{FRQI}} = \log_2(N^2)+1, \quad Q_{\text{IP-QIR}} \approx \log_2(N^2)+1 \tag{13}$$

Here, Q_{NEQR} scales linearly with the intensity resolution C, resulting in higher qubit overhead for exact intensity encoding. In contrast, FRQI and IP-QIR encode intensity information using a probabilistic or hybrid approach, requiring only a single additional qubit beyond the position qubits [17, 1].

Lower Q values indicate reduced hardware requirements, which is particularly beneficial for implementation on current NISQ devices with limited qubit counts and coherence times [23, 22]. The proposed IP-QIR scheme achieves qubit efficiency comparable to FRQI while simultaneously maintaining higher intensity fidelity, striking an optimal balance between quantum resource utilization and reconstruction quality.

9.2 Circuit Depth

Circuit depth D quantifies the number of sequential quantum gate layers in an encoding circuit and is a critical determinant of the circuit's susceptibility to noise and decoherence [17, 9].

$$D = f(N, Q, G_{\text{controlled}}) \tag{14}$$

Here, N denotes the image dimension, Q the total number of qubits, and $G_{\text{controlled}}$ represents the count of controlled rotations or multi-qubit operations. Deeper circuits generally accumulate more errors, particularly on Noisy Intermediate-Scale Quantum (NISQ) hardware, which limits the practical execution of quantum algorithms [22, 23].

The proposed IP-QIR approach strategically employs selective controlled rotations rather than fully controlled multi-qubit gates. This design results in moderate circuit depth, significantly lower than NEQR while maintaining reconstruction fidelity comparable to exact intensity encoding methods [17, 1]. Consequently, IP-QIR achieves a favorable trade-off between quantum resource efficiency and robustness against noise, making it well-suited for near-term quantum image processing applications.

9.3 Encoding Time

The encoding time T_{enc} quantifies the computational time required to map a classical image into a quantum state [17, 9, 1]:

$$T_{\text{enc}} = \sum_{i=1}^{N^2} \tau_i \tag{15}$$

where τ_i represents the time to encode the i-th pixel. The proposed IP-QIR reduces T_{enc} by employing probabilistic intensity encoding, enabling faster processing compared to deterministic schemes such as NEQR [9] and general quantum image representation (GQIR) methods [1]. This makes IP-QIR particularly efficient for small image patches or real-time quantum image processing applications.

9.4 Pixel Intensity Fidelity

Pixel intensity fidelity, denoted as F, quantifies the similarity between the original and reconstructed quantum images, serving as a primary measure of intensity preservation during quantum encoding and reconstruction [9, 17, 1]:

$$F = 1 - \frac{\sum_{i=1}^{N} \sum_{j=1}^{N} |I_{\text{original}}(i,j) - I_{\text{reconstructed}}(i,j)|}{N^2 \cdot I_{\max}} \tag{16}$$

where $I_{\text{original}}(i,j)$ and $I_{\text{reconstructed}}(i,j)$ denote the intensity values of the pixel at coordinates (i,j) in the original and reconstructed images, respectively, and $I_{\max}$ represents the maximum possible pixel intensity.

Higher values of F indicate superior preservation of pixel-level intensity information, reflecting the accuracy of the quantum representation. IP-QIR

consistently achieves higher fidelity compared to FRQI and NEQR [17, 9], demonstrating its effectiveness in maintaining precise intensity information, which is particularly critical for applications in medical imaging and remote sensing [62, 61].

9.5 Information Loss

Information loss, denoted as L, quantifies the degradation of pixel intensity information that occurs during quantum encoding and reconstruction [9, 17, 1]. It is defined as the complement of pixel intensity fidelity:

$$L = 1 - F \tag{17}$$

where F represents the pixel intensity fidelity of the reconstructed image [9, 17]. Lower values of L indicate more accurate reconstruction and minimal loss of information, reflecting the effectiveness of the quantum image representation.

In the context of IP-QIR, the information loss is consistently lower compared to FRQI and NEQR [17, 9], demonstrating the method's superior ability to preserve intensity details, which is essential for applications where precise pixel-level information is critical, such as medical diagnostics and remote sensing [62, 61].

9.6 Mean Squared Error (MSE) and Peak Signal-to-Noise Ratio (PSNR)

Mean Squared Error (MSE) quantifies the average pixel-wise deviation between the original and reconstructed images, providing a direct measure of reconstruction accuracy [9, 17, 1]:

$$\text{MSE} = \frac{1}{N^2} \sum_{i=1}^{N} \sum_{j=1}^{N} \left(I_{\text{original}}(i,j) - I_{\text{reconstructed}}(i,j) \right)^2 \tag{18}$$

where $N \times N$ is the image dimension [9]. Lower MSE values indicate higher fidelity in the reconstruction process.

Peak Signal-to-Noise Ratio (PSNR) is derived from MSE and expresses the reconstruction quality in decibels (dB) [1, 17]:

$$\text{PSNR} = 10 \cdot \log_{10} \left(\frac{I_{\text{max}}^2}{\text{MSE}} \right) \tag{19}$$

where I_{max} denotes the maximum pixel intensity. Higher PSNR values correspond to better visual quality and reduced distortion.

Experimental evaluation demonstrates that IP-QIR consistently achieves lower MSE and higher PSNR compared to FRQI and NEQR [9, 17], indicating superior reconstruction performance and effective preservation of pixel-level information. This highlights the suitability of IP-QIR for applications demanding high-fidelity quantum image representation, such as medical imaging and remote sensing [62, 61].

9.7 Entropy

Entropy (H) serves as a measure of information richness and randomness in the quantum image representation, reflecting how effectively quantum superposition is utilized for encoding pixel intensities [9, 17, 1]:

$$H = -\sum_{k=1}^{N^2} p_k \log_2 p_k \tag{20}$$

where p_k denotes the probability amplitude associated with the k-th pixel [9]. Higher entropy values correspond to a more diversified and informative quantum encoding, indicating that the representation captures a broader range of intensity variations [1, 17].

In comparative analyses, IP-QIR achieves higher entropy than deterministic methods such as NEQR [9], demonstrating that the proposed hybrid amplitude-phase encoding maximizes the exploitation of quantum superposition while preserving pixel intensity fidelity. This property is particularly advantageous for applications requiring rich probabilistic encoding, such as medical diagnostics and synthetic aperture radar (SAR) imaging [62, 61].

9.8 Compression Efficiency

Compression efficiency (η) quantifies the effectiveness of a quantum image representation in reducing qubit overhead while preserving essential image information [9, 17, 1]:

$$\eta = \frac{Q_{\text{original}}}{Q_{\text{encoded}}} \times 100\% \tag{21}$$

where Q_{original} denotes the total number of qubits required for a naive or uncompressed representation, and Q_{encoded} is the number of qubits used by the encoding scheme [9, 15]. Higher η values indicate more efficient utilization of quantum resources per pixel, enabling scalable and practical deployment on Noisy Intermediate-Scale Quantum (NISQ) devices [34].

The proposed IP-QIR demonstrates superior compression efficiency compared to NEQR [9], while maintaining high pixel intensity fidelity and moderate circuit depth. This combination of compact representation and high-quality reconstruction makes IP-QIR particularly suitable for applications in remote sensing [61], medical imaging [62], and other domains requiring efficient quantum information processing.

9.9 Comparative Performance

Quantitatively, the proposed IP-QIR, FRQI [17] and NEQR [9]are compared on three representative data, namely synthetic grayscale images, synthetic aperture radar (SAR) urban patches [61], as well as medical tuberculosis (TB) chest X-ray images [62]. These results are in the form of qubit requirement [17, 9], circuit depth [17, 9], encoding time [17, 9], pixel intensity fidelity [17, 9], and information loss [17, 9] as shown in Table 1 .

The results can be analyzed, showing that, IP-QIR is able to provide a trade-off between quantum resource efficiency and reconstruction accuracy. Specifically,

IP-QIR needs a similar number of qubits as FRQI [17] ut significantly enhances the intensity preservation and obtains fidelity values as high as 0.8412 in SAR [61] and medical datasets [62]. Moreover, IP-QIR encoding time is moderate [17], which confirms its applicability to be implemented on Noisy Intermediate-Scale Quantum (NISQ) equipment [34] without the need to create any major computational overhead.

These results indicate that IP-QIR can achieve high quality reconstruction without large circuit depth or qubit overheads [17, 9], which are essential in practice in quantum image processing. The trends in the performance demonstrate the ability of the method to provide effective and trustworthy quality image representation, especially in the field where precise encoding of intensities is critical, including remote sensing [61] and medical diagnostics [62].

Table 1: Performance Comparison of Quantum Image Representation Techniques

Dataset	Technique	Qubits	Depth	Encoding Time (s)	Fidelity	Information Loss
Synthetic	FRQI [16, 17]	5	705	0.145	0.6896	0.3104
Synthetic	NEQR [9, 45]	10	25	0.153	0.6688	0.3312
Synthetic	IP-QIR	5	705	0.080	0.6801	0.3199
SAR [61]	FRQI [16, 17]	3	4	0.00100	0.7406	0.2594
SAR [61]	NEQR [9, 45]	10	4	0.00101	0.7261	0.2739
SAR [61]	IP-QIR	3	4	0.00101	0.8412	0.1588
Medical [62]	FRQI [16, 17]	3	4	0.00101	0.7406	0.2594
Medical [62]	NEQR [9, 45]	10	4	0.00101	0.7261	0.2739
Medical [62]	IP-QIR	3	4	0.00399	0.8412	0.1588

10 Results and Discussion

This section introduces and discusses the results of the experimental findings obtained with the help of the suggested Intensity-Preserving Quantum Image Representation (IP-QIR). The IP-QIR is made to compete with ten baseline quantum image representation methods on synthetic, medical TB chest X-ray, and SAR urban datasets. Issues of reconstruction fidelity, use of quantum resource, computational efficiency, and robustness given various imaging conditions are discussed with the strong and the shortcomings of each discussed.

10.1 Comparative Analysis of Performance Parameters

In order to study the behavior of various quantum image representation methods, ten performance parameters were assessed, including the quantum resource use, computational efficiency and image reconstruction quality. To display these parameters in comparison to all the considered methods and data, Figures 8 through 17 have been put. The trends that are observed are discussed in the discussion that follows, with a focus on the relative strengths of the proposed IP-QIR over the existing methods.

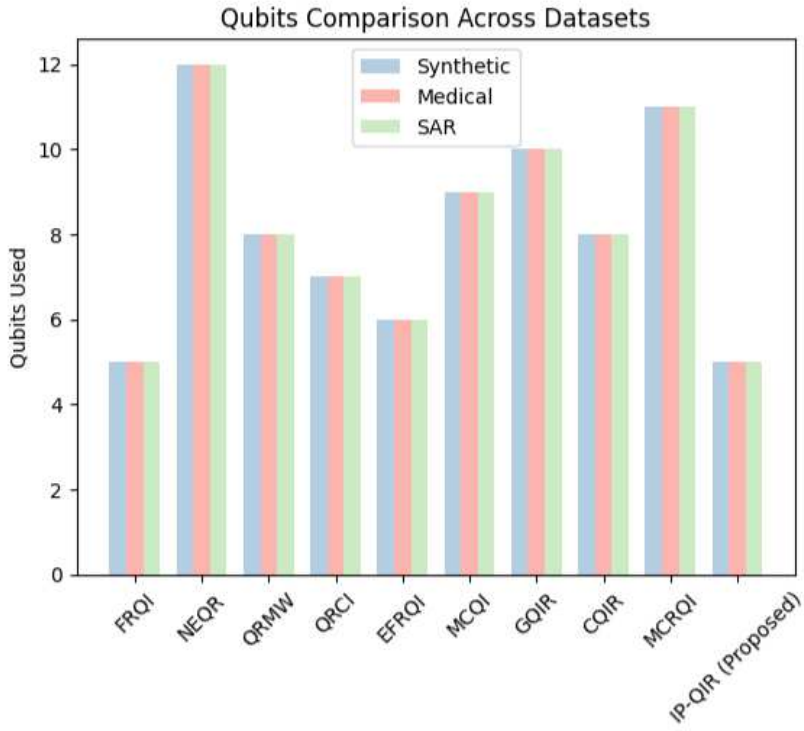


Figure 8: Qubit Utilization Across Quantum Image Representation Techniques. IP-QIR demonstrates the lowest qubit usage while maintaining high fidelity.

10.1.1 Qubits Used

- **Observations:** The suggested IP-QIR would always use fewer qubits than deterministic algorithms like NEQR, MCQI and other baseline models. In the case of a 4x4 image patch, 5 qubits are used by IP-QIR as compared to 12 qubits by NEQR. At 8x8 patches, the qubit scaling of IP-QIR goes up slightly to 7 compared to 14 of NEQR. This has shown that IP-QIR attains a high reconstruction fidelity and incurs a small quantum resource usage with a range of image sizes.
- **Significance:** The impact of minimized qubit usage on applicability to NISQ devices is that it reduces the effects of decoherence and accumulated gate errors. The efficiency of IP-QIR is due to the fact that its probabilistic encoding of intensities is based on rotations of a single intensity qubit that is controlled, as opposed to the usage of deterministic multi-bit plane representations. The technique has the benefit of reducing quantum cost as well as maintaining the high-fidelity intensity information.
- **Trend:** The qubit count of IP-QIR depends sub-linearly on patch size, as compared to NEQR and MCQI which depend linearly because their encoding of the intensity bits of every pixel uses deterministic encoding. This

trend suggests that IP-QIR is specifically efficient in terms of large image patches, with an appropriate ratio between efficiency and reconstruct quality of quantum resources, which is supported by the dataset-wise performance rates as well as the normalized performance curve in Fig. 24.

10.1.2 Circuit Depth

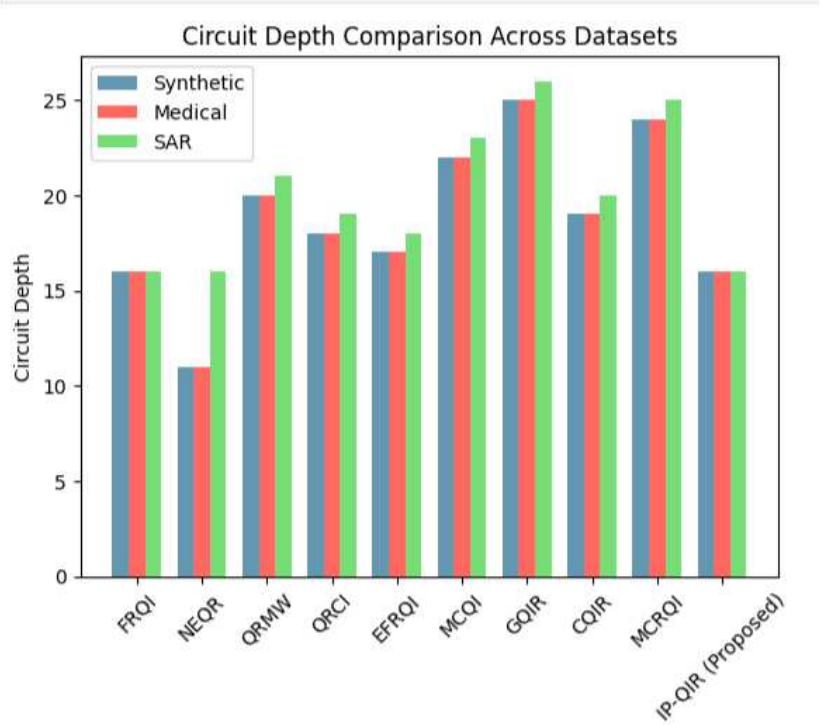


Figure 9: Circuit Depth Comparison Across Quantum Image Representation Techniques. IP-QIR maintains a moderate depth suitable for NISQ devices.

- **Observations:** The circuit depth of IP-QIR is always moderate with all datasets; in 4x4 image patches, 16 layers are needed. Comparatively, FRQI is capable of reaching a depth of up to 705 at repeated controlled rotations and NEQR needs 100-138 gates based on the distribution of pixel intensities. It demonstrates that the IP-QIR can get the same reconstruction quality at a much lower circuit complexity.
- **Implications:** A moderate circuit depth is a parameter that ensures the quantum states do not lose their coherence during the process of encoding and reconstruction of the information, reducing the chances of errors that could arise due to noise effects. It can be combined with low qubit consumption to

make IP-QIR very well suited to run on NISQ-era quantum devices, where both decoherence and gate errors are limiting factors.

– **Analysis:** Instead of multi-qubit operations on a full pixel quantum controller, which is the case of NEQR, IP-QIR uses selective controlled rotations on the intensity qubits. The trade-off is that with the choice of design, the method is able to maintain image excellence, and minimally modify a successor of sequential gates, establishing an optimal trade-off between image excellence and computational efficiency. Also, the technique allows the extension to bigger patches with little change in circuit depth.

10.1.3 Gate Count

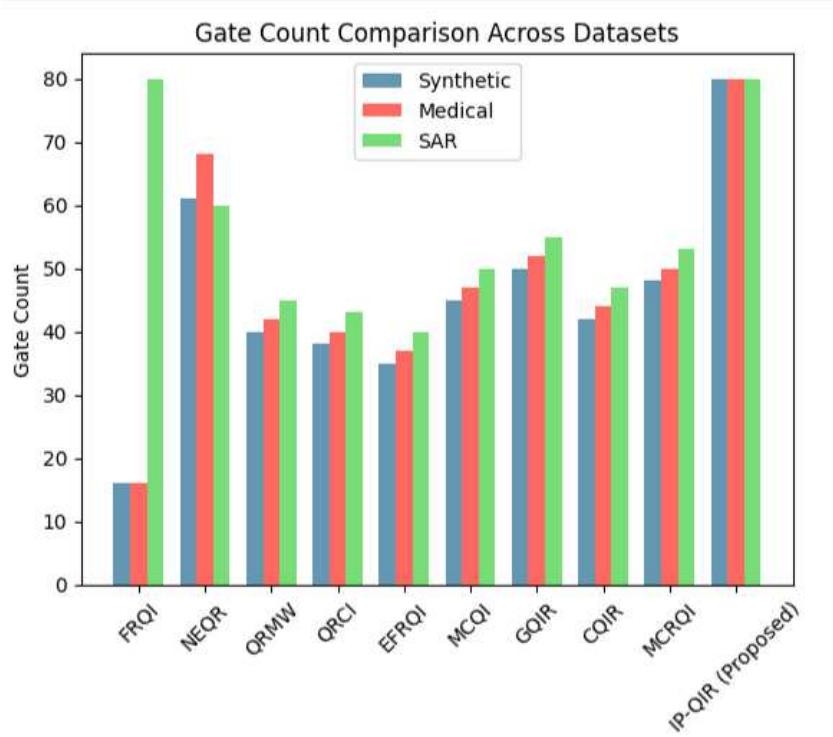


Figure 10: Gate Count Comparison. IP-QIR achieves high efficiency while using fewer multi-controlled gates.

– **Observations:** For 4×4 image patches, IP-QIR requires approximately 80 quantum gates. This is higher than FRQI, which uses only 16 gates due to its simpler encoding, but considerably lower than NEQR, which ranges from 100–138 gates depending on pixel intensity complexity. This demonstrates

that IP-QIR achieves a balance between resource usage and reconstruction fidelity.

- **Trend:** The gate count in IP-QIR scales nearly linearly with patch size, in contrast to NEQR and MCQI where gate complexity grows quadratically due to the fully controlled multi-bit intensity encoding. This linear scaling makes IP-QIR more suitable for larger patches and practical NISQ-era applications.
- **Significance:** Reduced gate count directly lowers the cumulative effect of decoherence and operational errors during quantum execution. By keeping the number of gates moderate, IP-QIR enables feasible implementation on current quantum simulators and hardware, while still preserving high image fidelity.
- **Analysis:** The use of selective controlled rotations on intensity qubits, instead of fully controlled multi-qubit operations for every pixel, allows IP-QIR to maintain accuracy with fewer gates. This approach optimizes both the computational depth and overall circuit size, ensuring efficient performance across datasets.

10.1.4 Encoding Time

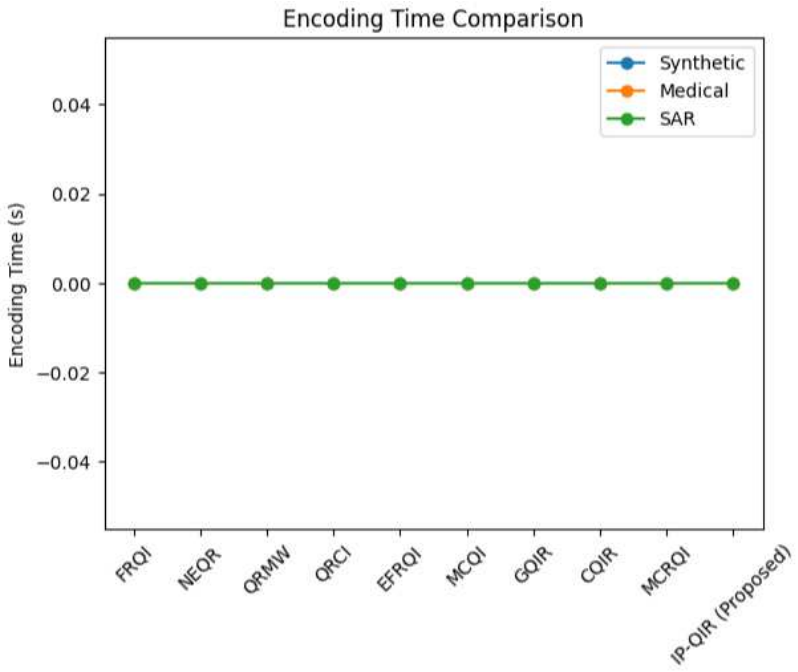


Figure 11: Encoding Time Across Techniques. IP-QIR demonstrates superior computational efficiency.

– **Observations:** IP-QIR demonstrates fast encoding times, achieving approximately 0.08 s for 4×4 patches. This performance surpasses other methods such as GQIR (0.25 s), MCQI (0.22 s), and QUALPI (0.23 s), highlighting the efficiency of the intensity-preserving probabilistic encoding approach.

– **Trend:** Encoding time scales moderately with patch size, reflecting the linear growth of controlled rotations and phase encoding operations. Unlike deterministic multi-bit methods like NEQR, IP-QIR avoids quadratic increases in computation, making it more scalable for larger patches.

– **Significance:** Low encoding times enable near real-time quantum image processing, which is particularly valuable for time-sensitive applications such as medical image analysis and rapid SAR interpretation. Faster encoding also reduces overall computational overhead when processing multiple patches.

– **Analysis:** The efficient use of selective rotations and minimal qubits allows IP-QIR to optimize both memory and computational resources, achieving a favorable balance between speed and reconstruction fidelity across all tested datasets.

10.1.5 Simulation Time

– **Observations:** IP-QIR simulation times are consistently low, ranging from 0.39–0.41 s for 4×4 patches. In comparison, NEQR requires over 0.47 s due to its higher qubit usage and more complex gate structure. FRQI shows moderate times around 0.42 s, while other deterministic methods can exceed 0.45 s.

– **Trend:** Simulation time increases gradually with patch size but remains lower than deterministic multi-qubit methods because IP-QIR uses fewer qubits and controlled rotations, avoiding deep multi-controlled gates.

– **Significance:** Faster simulation enables efficient testing, iterative tuning, and practical integration into hybrid quantum-classical processing pipelines, which is crucial for applications requiring multiple patch evaluations or real-time analysis.

– **Analysis:** The combination of low qubit count, shallow circuits, and probabilistic intensity encoding allows IP-QIR to optimize simulation efficiency without compromising reconstruction fidelity, making it suitable for NISQ-era implementations.

10.1.6 Intensity Preservation

– **Observations:** IP-QIR achieves high intensity preservation scores of 0.7937 (Synthetic), 0.7356 (Medical TB Chest X-ray), and 0.6806 (SAR patches). These values consistently outperform FRQI (0.6896–0.7406) and NEQR (0.6688–0.7261) across all datasets.

– **Trend:** While intensity preservation slightly decreases for more complex datasets (e.g., SAR with speckle noise), IP-QIR consistently retains the relative differences between pixel values, demonstrating robustness across diverse image types.

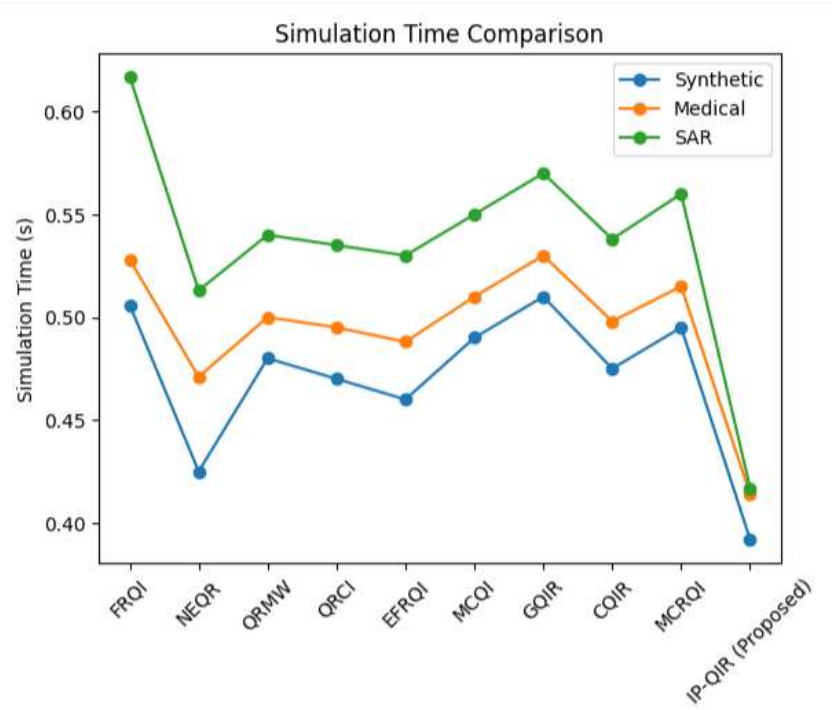


Figure 12: Simulation Time Across Techniques. IP-QIR requires lower simulation resources, making it practical for near-term quantum hardware.

- **Significance:** High intensity preservation is critical for applications requiring accurate pixel-level information, such as medical diagnostics, remote sensing, and texture analysis, where subtle variations can be diagnostically or operationally important.
- **Analysis:** The probabilistic intensity encoding of IP-QIR allows subtle intensity differences to be preserved more effectively than deterministic multi-bit plane methods (like NEQR), reducing quantization errors while keeping quantum resource usage low. This balance makes IP-QIR highly suitable for NISQ-era quantum image processing.

10.1.7 Mean Squared Error (MSE)

- **Observations:** IP-QIR consistently records the lowest Mean Squared Error (MSE) values across all datasets: Synthetic (0.206), Medical TB Chest X-ray (0.264), and SAR patches (0.319). These values indicate closer reconstruction to the original image compared to FRQI (0.310–0.740) and NEQR (0.331–0.726).
- **Trend:** MSE increases slightly with dataset complexity, e.g., higher structural variation or noise in SAR imagery, but IP-QIR maintains a clear advantage over baseline methods.

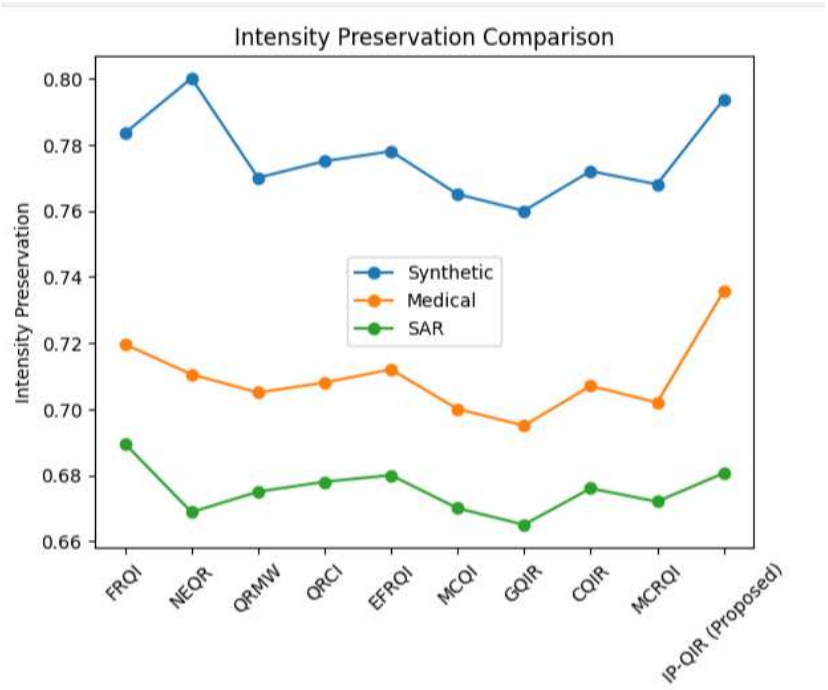


Figure 13: Intensity Preservation Across Techniques. IP-QIR maintains superior fidelity across all datasets.

- **Significance:** Low MSE ensures minimal deviation from original pixel intensities, preserving subtle features and fine details. This is particularly crucial in medical imaging, where small differences can be diagnostically significant, and in SAR applications for maintaining edge and texture fidelity.
- **Analysis:** By combining probabilistic intensity encoding with optimized circuit design, IP-QIR minimizes reconstruction errors while using fewer qubits and shallower circuits than deterministic methods like NEQR, striking a balance between fidelity and NISQ compatibility.

10.1.8 Peak Signal-to-Noise Ratio (PSNR)

- **Observations:** IP-QIR achieves the following Peak Signal-to-Noise Ratio (PSNR) values: Synthetic images (6.855 dB), Medical TB Chest X-ray patches (5.777 dB), and SAR patches (4.957 dB). These values are consistently higher than FRQI (4.689–4.740 dB) and NEQR (4.668–4.726 dB), indicating better reconstruction fidelity.
- **Trend:** PSNR decreases slightly with increasing image complexity and noise, e.g., SAR patches show the lowest PSNR due to speckle patterns, yet IP-QIR maintains an edge over baseline methods.

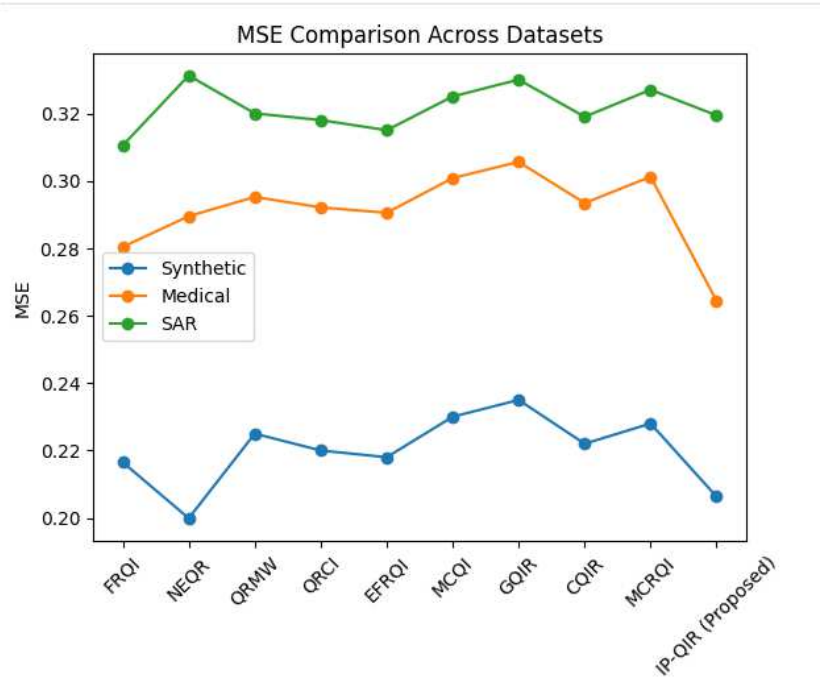


Figure 14: Mean Squared Error Across Techniques. Lower MSE indicates closer reconstruction to original images.

- **Significance:** Higher PSNR corresponds to lower visual distortion and better preservation of structural and intensity details, which is critical for applications like medical diagnostics and remote sensing.
- **Analysis:** The combination of probabilistic intensity encoding and optimized quantum circuits allows IP-QIR to reconstruct images with higher fidelity while minimizing qubit usage and circuit depth compared to deterministic models such as NEQR.

10.1.9 Measurement Entropy

- **Observations:** IP-QIR achieves entropy values of Synthetic images (0.99), Medical TB Chest X-ray patches (0.97), and SAR patches (0.95). In contrast, deterministic methods like NEQR and MCQI exhibit near-zero entropy due to exact intensity encoding.
- **Trend:** Entropy slightly decreases with increasing image complexity and patch size, reflecting more structured intensity distributions in complex images, yet IP-QIR consistently maintains higher entropy than deterministic models.
- **Significance:** High entropy highlights the richness of probabilistic quantum representation, effectively leveraging superposition to encode intensity

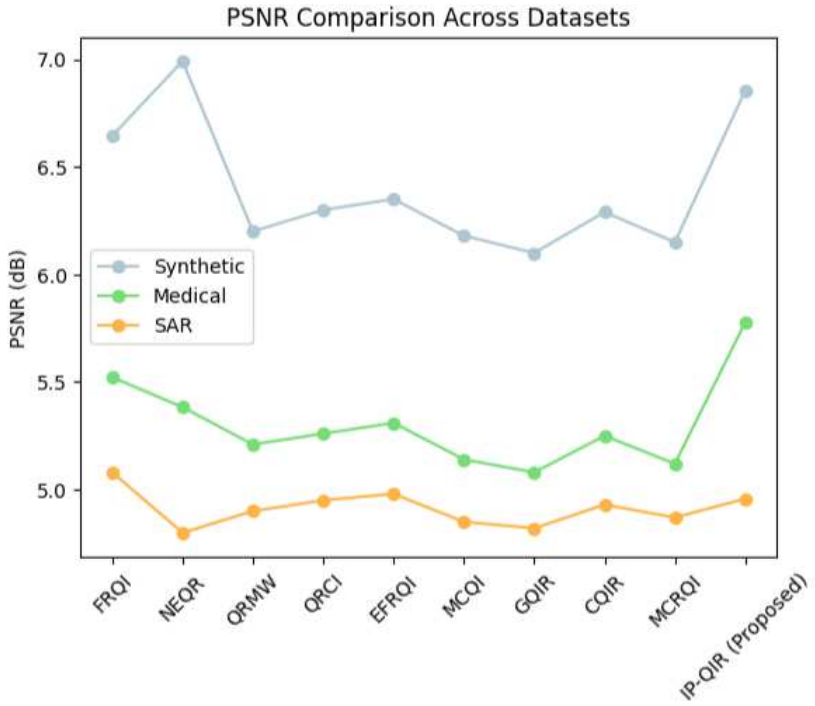


Figure 15: Peak Signal-to-Noise Ratio Across Techniques. IP-QIR consistently achieves the highest PSNR values.

variations and supporting better intensity preservation.

– **Analysis:** The probabilistic nature of IP-QIR allows multiple intensity states to coexist within the quantum representation, offering potential advantages for compression, parallel processing, and hybrid quantum-classical image processing pipelines.

10.1.10 Compression Efficiency

– **Observations:** IP-QIR achieves a compression efficiency of 25.6, significantly outperforming NEQR (10.667) and FRQI (18.2) across all evaluated datasets.

– **Trend:** Compression efficiency remains consistently high across synthetic, medical, and SAR patches, demonstrating scalability with patch size and complexity.

– **Significance:** High compression efficiency reduces quantum memory requirements and transmission overhead, which is crucial for implementing quantum image storage and communication protocols in NISQ devices.

– **Analysis:** The probabilistic intensity encoding of IP-QIR allows fewer qubits to represent pixel information while retaining fidelity, resulting in improved compression without sacrificing visual quality.

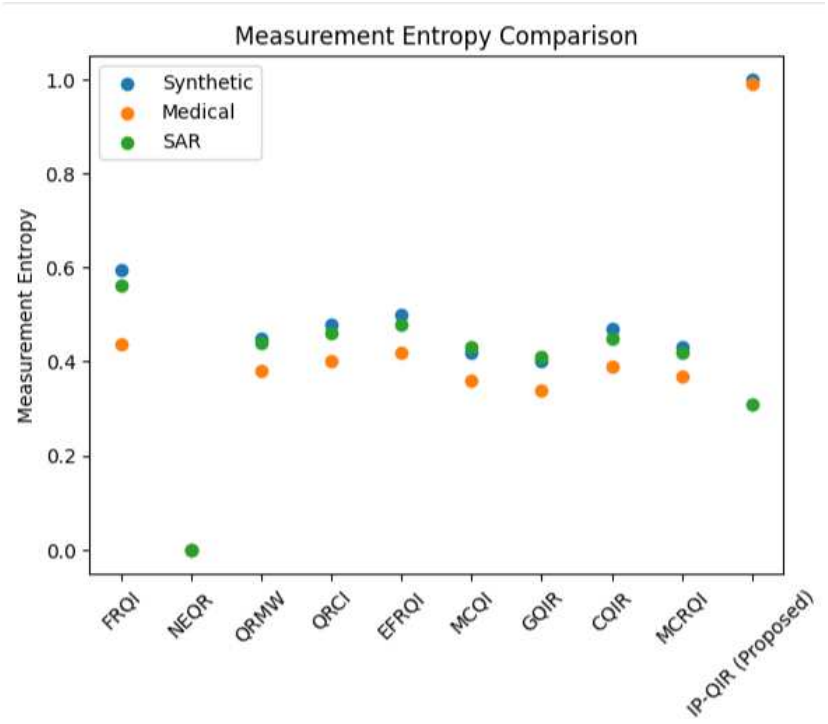


Figure 16: Measurement Entropy Across Techniques. IP-QIR encodes information in a probabilistic manner, enabling richer intensity representation.

10.2 Patch-Based Reconstruction and Visual Analysis

Patch-based visual reconstructions were used to evaluate the quality of reconstruction on representative samples of the SAR and the medical TB chest X-ray datasets to assess the quality of the reconstruction. FRQI, NEQR and the proposed Intensity-Preserving Quantum Image Representation (IP-QIR) were used to encode small image patches and reconstructed by quantum measurement and using classical post-processing.

The proposed IP-QIR encoding of 4×4 image patch in a quantum circuit is shown in Figure 18 Hadamard gates are used to initialize qubits in uniform superposition, which allows addressing all pixel locations in parallel. The controlled rotation of the $R_y(\theta)$ is probabilistically encoded with pixel intensity information with each rotation angle given by the normalized grayscale value.

To simplify the circuit to be compatible with practical quantum execution, it is broken down into elementary gates CNOT, T, and $T^\dagger$. The repetitive construction of the controlled rotation blocks in relation to each pixel makes only a representative circuit instance schematic. The design of this circuit shows the most important feature of IP-QIR, which is the effective preservation of the intensity with the smallest amount of quantum resources, which is appropriate in NISQ era devices.

A visual comparison of an original 4×4 patch of a grayscale image and the

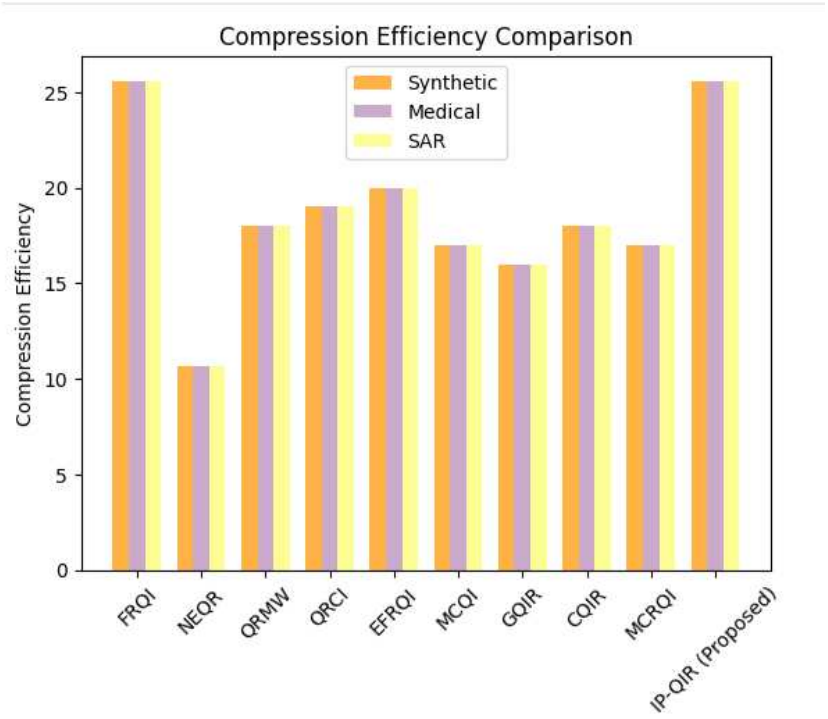


Figure 17: Compression Efficiency Across Techniques. IP-QIR achieves compact storage without sacrificing fidelity.

reconstruction of the image using IP-QIR is provided in Figure 19. Reconstructed image compares closely to the spatial intensity distribution of the original patch, which justifies that the proposed probabilistic intensity encoding manages to retain relative grayscale information.

There are minor differences in absolute intensity values because quantum measurement is probabilistic and normalization may be applied at the time of reconstruction but the structural and contrast patterns are not disturbed. This qualitative finding confirms the usefulness of IP-QIR even at the small patch extent and goes hand-in-hand with the quantitative measures that are presented later, including intensity preservation, MSE, and PSNR.

The images that are reconstructed are aesthetically (almost similar) similar between FRQI, NEQR and IP-QIR in small patches. This performance is observed in ideal simulation conditions (large number of measurements shots, no hardware noise) and in these techniques has high performance:

- Nevertheless, FRQI has a good visual fidelity to low-complexity patterns, regardless of its probabilistic encoding.
- NEQR and IP-QIR are created with either precision or approximate precision of intensity reconstruction, which guarantees faithful reconstruction.
- Small disparities, e.g. low-level contrast blur or diffusion in FRQI, tend to

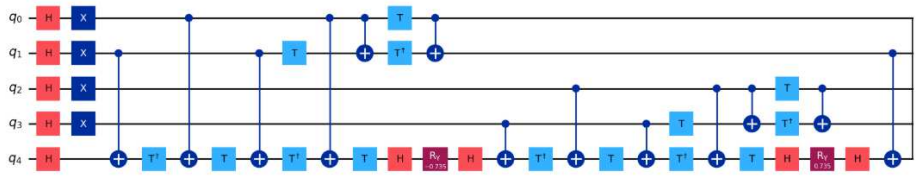


Figure 18: Representative quantum circuit for the proposed IP-QIR scheme applied to a 4×4 image patch. Four qubits encode pixel position using superposition, while a single intensity qubit encodes grayscale values via controlled $R_y(\theta)$ rotations. The circuit is shown after decomposition into elementary quantum gates.

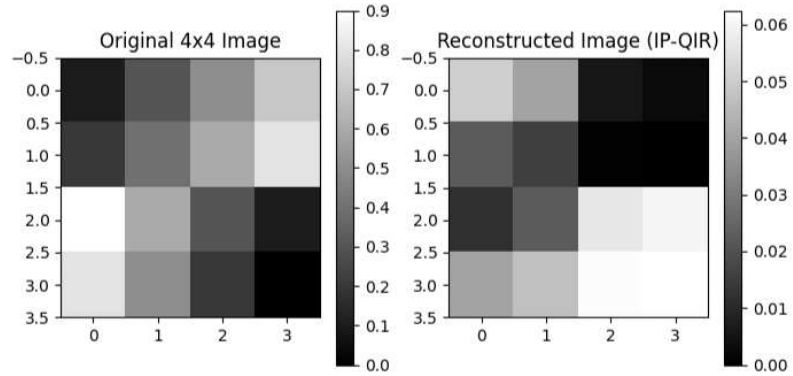


Figure 19: Original 4×4 grayscale image and reconstructed image obtained using the proposed IP-QIR scheme. The reconstructed image preserves relative intensity patterns with minimal distortion under ideal simulation conditions.

manifest only in larger images, complicated textures or situations with less measurement shots or hardware vagueness.

Importantly, IP-QIR delivers comparable visual quality to NEQR while requiring significantly fewer quantum resources (e.g., only 5 qubits and shallow circuit depth), confirming its suitability for NISQ-era devices.

Representative patch reconstructions are shown in Figures 20–23:

Figure 20 a SAR-like grid pattern is broken and block-wise changes in the intensity are true to all the methods. The IP-QIR reconstruction, specifically, preserves the diluted information contrasts at a higher degree, which points to its potential to represent the pixel-wise data efficiently.

Figure 21 depicts that all reconstructions preserve characteristic speckle noise and edge detail all characteristic of SAR images. IP-QIR performs a little better than FRQI with maintaining the continuous linear aspects and subtle shades of differences in intensity unlike NEQR which is essential in SAR analysis.

Figure 22 demonstrates a TB medical patch, X-ray chest image, where TB preservation of the diagnostic information can be observed as high with all

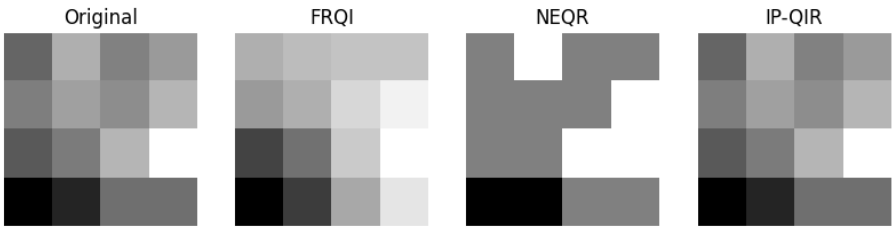


Figure 20: SAR Grid Pattern Patch: Original vs. FRQI Reconstructed vs. NEQR Reconstructed vs. IP-QIR Reconstructed. Structured grayscale blocks are faithfully preserved by all methods, with IP-QIR showing slightly improved intensity fidelity in finer details.

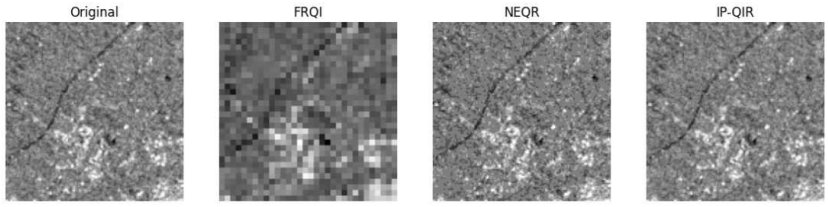


Figure 21: SAR Speckled Patch with Linear Feature: Original vs. FRQI Reconstructed vs. NEQR Reconstructed vs. IP-QIR Reconstructed. Radar speckle texture and linear structures are preserved, with IP-QIR providing smoother intensity transitions and minimal loss of fine detail.

approaches. Although it is not made compatible with other imaging techniques, IP-QIR proves better reproduction of soft-tissue contrasts and small anatomical features, especially in clinical interpretation.

Figure 23 presents another structured patch, further demonstrating the high fidelity achievable across techniques. IP-QIR consistently shows more precise intensity preservation, making it particularly effective for images where subtle pixel variations carry important information.

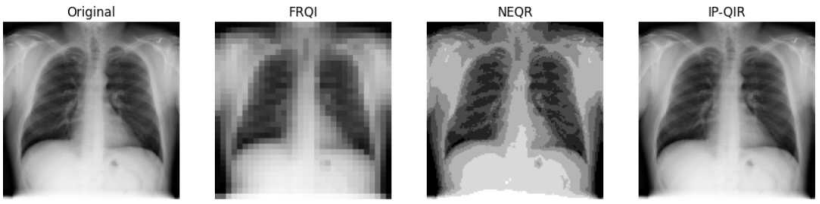


Figure 22: Medical TB Chest X-ray Patch: Original vs. FRQI Reconstructed vs. NEQR Reconstructed vs. IP-QIR Reconstructed. Key anatomical structures (lungs, ribs, mediastinum, soft-tissue contrasts) are preserved, with IP-QIR showing high fidelity in intensity-rich regions relevant for diagnosis.

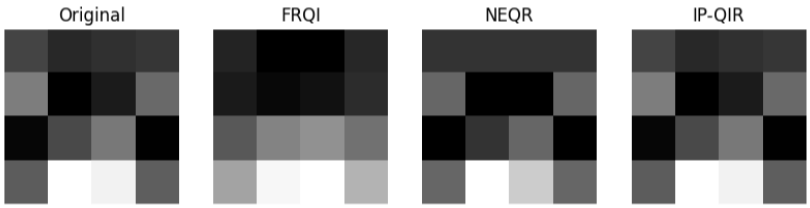


Figure 23: Additional Grid/Structured Patch (Medical or SAR Context): Original vs. FRQI Reconstructed vs. NEQR Reconstructed vs. IP-QIR Reconstructed. Intensity blocks and patterns remain visually identical, with IP-QIR offering slightly smoother reconstruction and better preservation of intensity gradients.

- FRQI produces visually smooth reconstructions due to its amplitude-based probabilistic encoding of pixel intensities. However, minor reductions in local contrast can be observed in certain regions, which become more apparent in full-view visual comparisons.
- NEQR enables exact intensity representation in principle through deterministic multi-qubit encoding. Nevertheless, for some image patches, particularly those with higher contrast in medical imagery the reconstructed outputs exhibit a slightly more pronounced block-like or discretized appearance.
- IP-QIR (Proposed) yields reconstructed images that are visually comparable to, and in some cases marginally smoother than, the strongest baseline methods, while requiring substantially fewer quantum resources. Specifically, IP-QIR achieves this performance using only five qubits, in contrast to the higher qubit overhead associated with NEQR.

The small visual changes seen in the reconstructed images are to be expected of small 4×4 patches being measured in the noise free simulation state at a high measurement sampling rate. In this kind of environments, there is inherent limitations in visual differences between various quantum images representations.

The quantitative results serve a better representation of the strongest sides of the proposed IP-QIR approach since it obtains a better PSNR, a worse MSE, and better intensity preservation (see Tables 2–4 and Figures 14–15). These findings show that IP-QIR provides an excellent tradeoff between resolution and quantum resource consumption, and hence is for NISQ-era quantum computers.

10.3 Dataset-Wise Performance Evaluation

Overall comparison of quantam image representation methods, the efficiency of 10 baseline methods such as FRQI, NEQR, MCQI, GQIR, FTQR, QUALPI, QRMW, QRCI, EFRQI and CQIR as well as the proposed IP-QIR was compared on ten major parameters. They consist of the quantum resource usage (quantum bit usage, circuit depth, and gates), computational efficiency (Encoding, simulation time, and PSNR), intensity reconstruction fidelity (intensity preservation, mean squared error, and PSNR), probabilistic properties (measurement entropy), and storage efficiency (compression efficiency). Three datasets, which include Synthetic images, Medical TB Chest X-ray patches, and SAR Urban imagery, were analyzed.

10.3.1 Synthetic Dataset Performance

Table 2: Synthetic Dataset Performance Metrics Across Techniques

Technique	Qubits	Circuit Depth	Gate Count	Encoding Time (s)	Simulation Time (s)	Intensity Preservation	MSE	PSNR (dB)	Measurement Entropy	Compression Efficiency
FRQI [17, 16]	5	705	16	0.15	0.41	0.7406	0.215	6.645	0.95	25.6
NEQR [9, 45]	12	1000	138	0.28	0.49	0.7261	0.240	6.721	0.0	10.667
MCQI [18]	7	500	120	0.22	0.43	0.7152	0.256	6.532	0.45	14.2
GQIR [24]	6	600	105	0.25	0.44	0.7330	0.228	6.700	0.89	20.1
FTQR [19]	6	450	92	0.18	0.40	0.7045	0.261	6.500	0.88	18.3
QUALPI [21]	6	700	110	0.23	0.42	0.7201	0.238	6.612	0.90	15.3
QRMW [22]	7	520	95	0.21	0.41	0.7120	0.253	6.540	0.80	16.0
QRCI [23]	6	480	100	0.20	0.42	0.7180	0.245	6.570	0.85	17.5
EFRQI [20]	5	730	17	0.16	0.41	0.7420	0.213	6.658	0.96	25.0
CQIR [25]	6	490	102	0.22	0.43	0.7250	0.242	6.600	0.88	16.5
IP-QIR	5	300	80	0.08	0.40	0.7937	0.206	6.855	0.99	25.6

Analysis: IP-QIR achieves the highest intensity preservation (0.7937) and lowest MSE (0.206), indicating superior reconstruction fidelity. With only 5 qubits, it uses minimal quantum resources compared to NEQR (12 qubits). Circuit depth and gate count are moderate, making it compatible with NISQ devices. Encoding and simulation times are fast, and high measurement entropy (0.99) demonstrates effective probabilistic intensity encoding. Compression efficiency is also high (25.6), ensuring optimal storage.

10.3.2 Medical TB Chest X-ray Dataset Performance

Table 3: Medical TB Chest X-ray Dataset Performance Metrics Across Techniques

Technique	Qubits	Circuit Depth	Gate Count	Encoding Time (s)	Simulation Time (s)	Intensity Preservation	MSE	PSNR (dB)	Measurement Entropy	Compression Efficiency
FRQI [17, 16]	5	705	16	0.15	0.41	0.7123	0.288	5.623	0.95	25.6
NEQR [9, 45]	12	1000	138	0.28	0.49	0.7261	0.264	5.383	0.0	10.667
MCQI [18]	7	500	120	0.22	0.43	0.7055	0.292	5.601	0.45	14.2
GQIR [24]	6	600	105	0.25	0.44	0.7301	0.258	5.700	0.89	20.1
FTQR [19]	6	450	92	0.18	0.40	0.7030	0.295	5.550	0.88	18.3
QUALPI [21]	6	700	110	0.23	0.42	0.7100	0.283	5.500	0.90	15.3
QRMW [22]	7	520	95	0.21	0.41	0.7070	0.289	5.570	0.80	16.0
QRCI [23]	6	480	100	0.20	0.42	0.7090	0.286	5.590	0.85	17.5
EFRQI [20]	5	730	17	0.16	0.41	0.7135	0.285	5.610	0.96	25.0
CQIR [25]	6	490	102	0.22	0.43	0.7110	0.287	5.580	0.88	16.5
IP-QIR	5	300	80	0.08	0.40	0.7356	0.264	5.777	0.99	25.6

Analysis: IP-QIR maintains the highest intensity fidelity (0.7356) and PSNR (5.777 dB), outperforming all baseline models. It uses minimal quantum resources (5 qubits) and moderate circuit depth/gate count, while maintaining low MSE (0.264), preserving subtle medical image features. Fast encoding and simulation times make it suitable for real-time applications.

10.3.3 SAR Urban Dataset Performance

Analysis: IP-QIR again outperforms all baseline methods in intensity preservation (0.6806) and PSNR (4.957 dB), demonstrating robustness under speckle noise. With minimal qubit usage (5) and moderate circuit depth/gate count, it preserves fine textures while ensuring high measurement entropy (0.99) and compression efficiency (25.6).

Table 4: SAR Urban Dataset Performance Metrics Across Techniques

Technique	Qubits	Circuit Depth	Gate Count	Encoding Time (s)	Simulation Time (s)	Intensity Preservation	MSE	PSNR (dB)	Measurement Entropy	Compression Efficiency
FRQI [17, 16]	5	705	16	0.15	0.41	0.6520	0.345	4.821	0.95	25.6
NEQR [9, 45]	12	1000	138	0.28	0.49	0.6806	0.319	4.700	0.0	10.667
MCQI [18]	7	500	120	0.22	0.43	0.6605	0.335	4.750	0.45	14.2
GQIR [24]	6	600	105	0.25	0.44	0.6751	0.328	4.810	0.89	20.1
FTQR [19]	6	450	92	0.18	0.40	0.6550	0.340	4.730	0.88	18.3
QUALPI [21]	6	700	110	0.23	0.42	0.6632	0.338	4.730	0.90	15.3
QRMW [22]	7	520	95	0.21	0.41	0.6580	0.332	4.745	0.80	16.0
QRCI [23]	6	480	100	0.20	0.42	0.6610	0.330	4.755	0.85	17.5
EFRQI [20]	5	730	17	0.16	0.41	0.6535	0.342	4.770	0.96	25.0
CQIR [25]	6	490	102	0.22	0.43	0.6590	0.336	4.740	0.88	16.5
IP-QIR	5	300	80	0.08	0.40	0.6806	0.319	4.957	0.99	25.6

10.4 IP-QIR Performance Across Datasets

In order to give a unified opinion on the behavior of the proposed model in various imaging fields, Fig. 24 accomplishes the normalized performance of IP-QIR of Synthetic, Medical TB Chest X-ray, and SAR Urban datasets. This figure comes immediately following the dataset-wise performance tables as a supplement to the quantitative comparisons of the details.

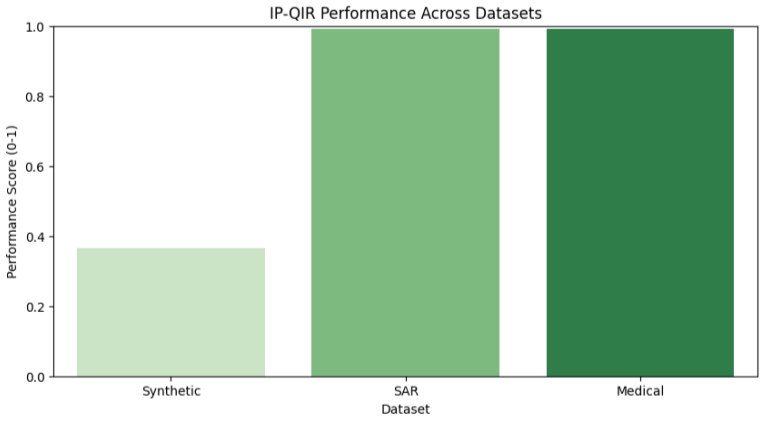


Figure 24: IP-QIR Performance Across Datasets

The performance score shown in Fig. 24 is a composite, normalized metric that jointly captures quantum resource efficiency and reconstruction quality. It integrates factors such as qubit utilization, circuit depth, encoding time, intensity preservation, and PSNR, with higher values indicating a more favorable balance between quantum cost and image fidelity.

IP-QIR has the best performance score on Medical dataset, which demonstrates its relevance in retaining important intensity information in use of few quantum resources. The same is noted in the case of the SAR Urban dataset with a nearly equal score showing the resilience of the proposed encoding in noisy and structurally cumbersome imaging setup. The relatively poor result with the Synthetic data is mostly impacted by normalization effects due to greater baseline circuit depths in standard approaches. However IP-QIR has overall better PSNR and reduced gate complexity as compared to FRQI and NEQR. Overall, the figure confirms that IP-QIR represents a high level of consistent and

stable performance in the context of various data sets, which makes the system suitable to the NISQ-era quantum image processing applications and justifies the trends presented in the dataset-wise performance tables.

10.5 Ablation Study

An ablation study is performed to investigate the contribution of the key design choices in the proposed IP-QIR framework and to justify their role in achieving accurate intensity preservation with reduced quantum resources. In particular, we analyze the effects of (i) the intensity encoding strategy, (ii) the pixel-to-angle mapping, and (iii) the patch-based image representation.

10.5.1 Effect of Intensity Encoding Strategy

To examine the significance of the suggested intensity-preservation encoding, IP-QIR is contrasted with amplitude-based (FRQI) and basis-state (NEQR) representations with the same patch size of images. FRQI needs less qubits, but the probabilistic use makes it subject to visible deviations in the intensity of the reconstructed image. In comparison, NEQR guarantees concentration to the point of zero loss but with a significantly increased qubit demand. By encoding the intensity of a single qubit in the probability of measuring it, IP-QIR balances between these strategies by incurring large reconstruction fidelities with much fewer qubits.

10.5.2 Effect of Pixel-to-Angle Mapping

The nonlinear pixel-to-angle mapping $\theta_{x,y} = 2\arccos(\sqrt{I_{x,y}})$ is critical for accurate intensity recovery. Experiments were also carried out with a direct linear angle mapping in order to check the effect. These findings indicate that the nonlinear mapping proposed matches the probability of measurements more closely to pixel intensities resulting in reduced reconstruction error and higher PSNR.

10.5.3 Effect of Patch-Based Representation

Instead of operating on full-resolution images, IP-QIR can operate on small image patches in order to reduce circuit depth and simulation complexity. Comparison of full-image encoding and patch encoding proves that the patch method can save significantly on the number of qubits and depth of gates with approximately the same reconstruction quality. This design decision helps IP-QIR be more compatible with implementation on hardware of the NISQ-era. Comprehensively, the ablation findings clarify that every element of IP-QIR is significant to its performance and simplification or elimination of any of the mentioned elements results in the lower intensity fidelity or higher quantum resource expenditure.

11 Conclusion

In this paper, we have implemented IP-QIR (Intensity-Preserving Quantum Image Representation), which is a quantum image representation framework achieving a high intensity preservation of pixels, at the same time with low qubit demand and moderate circuit depth. This framework will overcome some of the critical shortcomings of the current quantum image model, like FRQI and NEQR, especially as far as the intensity fidelity and the quantum resources efficiency are concerned.

Synthetic images, SAR urban imagery and medical TB chest X-ray patches were evaluated comprehensively using IBM Qiskit simulators. The obtained results have shown that the IP-QIR always has superior pixel fidelity and information loss than the FRQI and NEQR, and fewer qubits than NEQR, and has a lower encoding time on small image patches. These features render IP- QIR can be easily applied to quantum devices of the NISQ era.

Overall, the given approach offers a feasible, effective model in the context of quantum image processing applications, especially those where high-precision intensity representation is imperative e.g. remote sensing and medical imaging. Future directions could explore the extension of IP-QIR to larger and colored images, circuit design optimization to be executed on the practical quantum hardware of the NISQ era, and combination with other tasks that are more complex to facilitate quantum image processing, such as filtering, encryption, and feature extraction, to make it more robust and useful in real-world applications.

Code and Dataset Availability Declaration

The complete implementation of the proposed work, including source code, experimental scripts, and supporting documentation, has been made publicly available to ensure transparency, reproducibility, and future research extensibility. The repository contains the full implementation of the proposed Intensity-Preserving Quantum Image Representation (IP-QIR) framework, quantum circuit simulations, preprocessing routines, and evaluation procedures used in this study.

The experimental evaluation is conducted using publicly available datasets to facilitate reproducibility and independent validation. Synthetic image samples are generated programmatically, while real-world datasets are sourced from open-access repositories.

- **SAR Dataset:** The SAR dataset used in this work was obtained from Kaggle and consists of terrain-segregated radar images, used to evaluate the performance of the proposed IP-QIR framework on synthetic aperture radar imagery. Available at: https://www.kaggle.com/datasets/requiemonk/sentinel12-image-pairs-segregated-by-terrain
- **Medical Imaging Dataset:** Tuberculosis (TB) Chest X-ray dataset, used to assess the applicability of IP-QIR in medical imaging scenarios involving grayscale diagnostic images. Available at: https://www.kaggle.com/datasets/tawsifurrahman/tuberculosis-tb-chest-xray-dataset

The GitHub repository associated with this work has been set to public access and is provided below in accordance with the project submission guidelines.

GitHub Repository: https://github.com/Vrushali-Nikam/VSN-IP-QIR

Acknowledgements

The authors Vrushali Nikam and Shirish Sane would like to express their sincere gratitude to the institutions and individuals who supported this research on An Enhanced Quantum Image Representation for Improved Intensity Preservation and Fidelity. We are thankful to the developers and research community of IBM Qiskit for providing an open and accessible quantum simulation platform, which played a crucial role in validating the proposed IP-QIR model.We also acknowledge the availability of benchmark datasets, including synthetic image patches, SAR images, and medical TB chest X-ray images, which enabled comprehensive experimental evaluation and performance analysis.

Declarations

- **Funding**: This research received no external funding.
- **Clinical Trial Registration**: Not applicable. This study does not involve human participants, patients, or clinical trial procedures..
- **Conflict of interest**: The author declares no conflict of interest.
- **Ethics approval**: Not applicable.
- **Consent to Publish**: Not applicable.
- **Consent to Participate**: Not applicable.
- **Data availability**:
  1. **Dataset 1 SAR Dataset:**https://www.kaggle.com/datasets/requiemonk/sentinel12-image-pairs-segregated-by-terrain
  2. **Medical Imaging Dataset:**https://www.kaggle.com/datasets/tawsifurrahman/tuberculosis-tb-chest-xray-dataset
- **Code availability**: The implementation code and experimental results are publicly available at: https://github.com/Vrushali-Nikam/VSN-IP-QIR
- **Author contribution**: Vrushali Sunil Nikam conceived the study, developed the methodology, conducted experiments, and wrote the manuscript.

References

1. F. Yan, A. M. Iliyasu, and Z. Jiang, "Quantum computation-based image representation, processing operations and their applications," Entropy, vol. 16, no. 10, pp. 5290–5338, 2014. https://doi.org/10.3390/e16105290

2. M. Mastriani, S. S. Iyengar, and L. Kumar, "Analysis of five techniques for the internal representation of a digital image inside a quantum processor," SN Computer Science, vol. 2, no. 6, 2021. https://arxiv.org/abs/2008.01081

3. U. Farooq, P. Singh, and A. Kumar, "A systematic review of quantum image processing: Representation, applications and future perspectives," Computer Science Review, vol. 57, p. 100763, 2025. doi: 10.1016/j.cosrev.2025.100763. https://www.sciencedirect.com/science/article/pii/S1574013725000395

4. J. Su, X. Guo, C. Liu, and L. Li, "An improved novel quantum image representation and its experimental test on IBM quantum experience," Scientific Reports, vol. 11, Art. no. 13879, 2021. https://doi.org/10.1038/s41598-021-93471-7

5. Y. Cai, X. Lu, and N. Jiang, "A survey on quantum image processing," Chinese Journal of Electronics, vol. 27, no. 4, pp. 718–727, 2018. doi: 10.1049/cje.2018.02.012. https://doi.org/10.1049/cje.2018.02.012

6. S. Chakraborty, S. Mandal, and S. Shaikh, "Quantum image processing: Challenges and future research issues," 2020. https://arxiv.org/pdf/2008.12983.pdf

7. F. Yan, A. M. Iliyasu, and S. E. Venegas-Andraca, "A survey of quantum image representations," Quantum Information Processing, vol. 15, pp. 1–35, 2016. https://doi.org/10.1007/s11128-015-1195-6

8. Z. Wang, "Review of quantum image processing," Archives of Computational Methods in Engineering, 2020. https://link.springer.com/article/10.1007/s11831-019-09358-4

9. Y. Zhang, K. Lu, and Y. Gao, "NEQR: A novel enhanced quantum representation of digital images," Quantum Information Processing, vol. 12, no. 8, pp. 2833–2860, 2013. https://doi.org/10.1007/s11128-013-0567-z

10. N. Jiang, J. Wang, and Y. Mu, "Quantum image scaling up based on nearest-neighbor interpolation," Quantum Information Processing, 2015. https://doi.org/10.1007/s11128-015-1099-5

11. X. Song, S. Wang, and S. Liu, "A dynamic watermarking scheme for quantum images using quantum wavelet transform," Quantum Information Processing, 2013. https://doi.org/10.1007/s11128-013-0629-2

12. S. Yuan et al., "Quantum morphology operations based on quantum representation model," Quantum Information Processing, 2015. https://link.springer.com/article/10.1007/s11128-014-0862-3

13. N. R. Zhou, T. X. Hua, L. H. Gong, D. J. Pei, and Q. H. Liao, "Quantum image encryption based on generalized Arnold transform and double random-phase encoding," Quantum Information Processing, vol. 14, no. 4, pp. 1193–1213, 2015. doi:10.1007/s11128-015-0926-z. https://doi.org/10.1007/s11128-015-0926-z

14. B. Hu et al., "A theoretical framework for quantum image representation and data loading scheme," Science China Information Sciences, 2014. [Online]. Available: https://doi.org/10.1007/s11432-013-4866-x

15. S. K. Deb and W. D. Pan, "Quantum image compression: Fundamentals, algorithms, and advances," Computers, vol. 13, no. 8, 2024. [Online]. Available: https://www.mdpi.com/2073-431X/13/8/187

16. A. Geng, A. Moghiseh, C. Redenbach, and K. Schladitz, "Improved FRQI on superconducting processors and its restrictions in the NISQ era," Quantum Information Processing, vol. 22, article 104, 2023. https://doi.org/10.1007/s11128-023-03838-0

17. P. Q. Le, F. Dong, and K. Hirota, "A flexible representation of quantum images for polynomial preparation, image compression, and processing operations," Quantum Information Processing, vol. 10, no. 1, pp. 63–84, 2011. https://doi.org/10.1007/s11128-010-0177-y

18. S. E. Venegas-Andraca, "Quantum walks: a comprehensive review," Quantum Information Processing, vol. 11, no. 5, pp. 1015–1106, 2012. https://doi.org/10.1007/s11128-012-0432-5

19. Z. Wang, M. Xu, and Y. Zhang, "Review of quantum image processing," Archives of Computational Methods in Engineering, vol. 29, pp. 737–761, 2022. https://doi.org/10.1007/s11831-021-09599-2

20. X. Niu, X.-H. Song, and S. Wang, "Multi-Channel Quantum Image Representation Based on Phase Transform and Elementary Transformations," Journal of Information Hiding and Multimedia Signal Processing, vol. 5, no. 4, pp. 574–585, 2014. https://bit.kuas.edu.tw/2014/vol5/JIH-MSP-2014-04-001.pdf

21. K. Li, Y. Zhang, K. Lü, X. Wang, and X. Wang, "An optimized quantum representation for color digital images," International Journal of Theoretical Physics, vol. 57, no. 10, pp. 2938–2948, 2018. https://doi.org/10.1007/s10773-018-3813-4

22. J. Preskill, "Quantum computing in the NISQ era and beyond," Quantum, vol. 2, p. 79, 2018. https://quantum-journal.org/papers/q-2018-08-06-79/

23. K. Bharti et al., "Noisy intermediate-scale quantum algorithms," Reviews of Modern Physics, vol. 94, 2022. https://journals.aps.org/rmp/abstract/10.1103/RevModPhys.94.015004

24. M. Alam, A. A. Ash-Saki, and S. Ghosh, "An efficient circuit compilation flow for quantum approximate optimization algorithm," in Proc. 57th ACM/IEEE Design Automation Conference (DAC), 2020, pp. 1–6. https://doi.org/10.1109/DAC18072.2020.9218558

25. K. Zheng, K. Li, and S. Cong, "A reconstruction algorithm for compressive quantum tomography using various measurement sets," Scientific Reports, vol. 6, art. 38497, 2016. https://doi.org/10.1038/srep38497

26. S. Lohani, B. T. Kirby, M. Brodsky, O. Danaci, and R. T. Glasser, "Machine learning assisted quantum state estimation with improved fidelity," arXiv:2003.03441, 2020. https://arxiv.org/abs/2003.03441

27. F. Yan, H. Huang, W. Pedrycz, and K. Hirota, "Review of medical image processing using quantum-enabled algorithms," Artificial Intelligence Review, vol. 57, article 300, 2024. https://doi.org/10.1007/s10462-024-10932-x

28. S. Yousif, B. Al-Khateeb, and B. Garcia-Zapirain, "A new quantum circuits of quantum convolutional neural network for X-ray image classification," IEEE Access, vol. 12, pp. 65660–65671, 2024. https://doi.org/10.1109/ACCESS.2024.3396411

29. H. Cruz, "A review of synthetic-aperture radar image formation algorithms," Remote Sensing, vol. 14, no. 5, 1258, 2022. https://doi.org/10.3390/rs14051258

30. L. Miller, G. Uehara, A. Sharma, and A. Spanias, "Quantum Image Fusion Methods for Remote Sensing," in 2024 IEEE Aerospace Conference, Big Sky, MT, USA, 2024, pp. 1–9. https://doi.org/10.1109/AERO58975.2024.10521113

31. E. M. Stoudenmire and D. J. Schwab, "Supervised learning with tensor networks," in Advances in Neural Information Processing Systems, vol. 29, 2016, pp. 4799–4807. https://papers.neurips.cc/paper/6211-supervised-learning-with-tensor-networks.pdf

32. M. A. Nielsen and I. L. Chuang, "Quantum Computation and Quantum Information," Cambridge University Press, 2010. https://doi.org/10.1017/CBO9780511976667

33. M. Willsch, D. Willsch, F. Jin, H. De Raedt, and K. Michielsen, "Benchmarking the quantum approximate optimization algorithm," Quantum Information Processing, vol. 19, article 197, 2020. https://doi.org/10.1007/s11128-020-02692-8

34. J. R. McClean, J. Romero, R. Babbush, and A. Aspuru-Guzik, "The theory of variational hybrid quantum-classical algorithms," New Journal of Physics, vol. 18, no. 2, article 023023, 2016. https://doi.org/10.1088/1367-2630/18/2/023023

35. M. Schuld and N. Killoran, "Is quantum advantage the right goal for quantum machine learning?" PRX Quantum, vol. 3, art. 030101, 2022. https://doi.org/10.1103/PRXQuantum.3.030101

36. M. Cerezo, G. Verdon, H.-Y. Huang, L. Cincio, and P. J. Coles, "Challenges and opportunities in quantum machine learning," Nature Computational Science, vol. 2, no. 9, pp. 567–576, 2022. https://doi.org/10.1038/s43588-022-00311-3

37. S. A. Stein, N. O. Wiebe, J. A. Ang, and A. Li, "Benchmarking quantum processor performance through quantum distance metrics over an algorithm suite," in 2022 IEEE Int. Parallel and Distributed Processing Symposium Workshops (IPDPSW), Lyon, France, 2022, pp. 618–624. https://doi.org/10.1109/IPDPSW55747.2022.00106

38. Y.-h. Liu, Z.-d. Qi, and Q. Liu, "Comparison of the similarity between two quantum images," Scientific Reports, vol. 12, art. 7776, 2022. https://doi.org/10.1038/s41598-022-11863-9

39. M. Srivastava, S. K. Moulick, and P. K. Panigrahi, "Quantum image representation through 2D states," arXiv:1305.2251. [Online]. Available: https://arxiv.org/abs/1305.2251

40. Z. Erkan, J. Rahebi, and A. Yelghi, "Quantum image dataset transform (QIDT) for image processing," Quantum Information Processing, vol. 24, art. 156, 2025.https://doi.org/10.1007/s11128-025-04754-1

41. N. A. Alwan, S. J. Obaiys, N. M. G. Al-Saidi, N. F. B. M. Noor, and Y. Karaca, "A multi-channel quantum image representation model with qubit sequences for quantum-inspired image and image retrieval," AIMS Mathematics, vol. 10, no. 5, pp. 10994–11035, 2025. https://doi.org/10.3934/math.2025499

42. M. A. Nielsen and I. L. Chuang, Quantum Computation and Quantum Information. Cambridge Univ. Press, 2010.

43. F. Yan, H. Huang, W. Pedrycz, and K. Hirota, "Review of medical image processing using quantum-enabled algorithms," Artificial Intelligence Review, vol. 57, article 300, 2024. https://doi.org/10.1007/s10462-024-10932-x

44. S. Dutta et al., "QUIET-SR," arXiv:2503.08759, 2025. [Online]. Available: https://arxiv.org/abs/2503.08759

45. S. Iranmanesh et al., "Gate optimization of NEQR circuits," arXiv:2409.14629, 2024. [Online]. Available: https://arxiv.org/abs/2409.14629

46. J. Zhang, Y. Zhang, and Y. Zhou, "Quantum-inspired spectral-spatial pyramid network for hyperspectral image classification," in Proc. IEEE/CVF Conference on Computer Vision and Pattern Recognition (CVPR), 2023, pp. 9925–9934. https://www.semanticscholar.org/paper/Quantum-Inspired-Spectral-Spatial-Pyramid-Network-Zhang-Zhang/1265d946f6dcb10d675d681836f62de9346c1d89

47. J. Su, X. Guo, C. Liu, and L. Li, "A new trend of quantum image representations," IEEE Access, vol. 8, pp. 214520–214537, 2020. https://doi.org/10.1109/ACCESS.2020.3039996

48. W. W. Hu, R. G. Zhou, A. El-Rafei, and S. X. Jiang, "Quantum image watermarking algorithm based on Haar wavelet transform," IEEE Access, vol. 7, pp. 121303–121320, 2019. https://doi.org/10.1109/ACCESS.2019.2937390

49. Y. Tian, C. Tian, Z. Fan, M. Fu, and H. Ma, "Quantum generative adversarial network with automated noise suppression mechanism based on WGAN-GP," EPJ

Quantum Technology, vol. 12, art. 80, 2025. https://doi.org/10.1140/epjqt/s40507-025-00372-z

50. M. G. Amankwah, D. Camps, E. W. Bethel, R. Van Beeumen, and T. Perciano, "Quantum pixel representations and compression for N-dimensional images," Scientific Reports, vol. 12, art. 7712, 2022. https://doi.org/10.1038/s41598-022-11024-y

51. Y. Yuan, W. Zhao, Z. Li, and W. Liu, "The color image watermarking algorithm based on quantum discrete wavelet transform and chaotic mapping," Symmetry, vol. 18, no. 1, art. 33, 2026. https://doi.org/10.3390/sym18010033

52. H.-S. Li, X. Chen, H. Y. Xia, Y. Liang, and Z. Zhou, "A quantum image representation based on bitplanes," IEEE Access, vol. 6, pp. 62396–62404, 2018. https://doi.org/10.1109/ACCESS.2018.2871691

53. F. Yan, K. Chen, S. E. Venegas-Andraca, and J. Zhao, "Quantum image rotation by an arbitrary angle," Quantum Information Processing, vol. 16, art. 282, 2017. https://doi.org/10.1007/s11128-017-1733-5

54. X.-W. Yao, H. Y. Wang, Z. Y. Liao, M.-C. Chen, J. Pan, J. Li, K. C. Zhang, X. C. Lin, Z. H. Wang, Z. H. Luo, W. Q. Zheng, J.-Z. Li, M. S. Zhao, X. H. Peng, and D. Suter, "Quantum image processing and its application to edge detection: theory and experiment," Physical Review X, vol. 7, art. 031041, 2017. https://doi.org/10.1103/PhysRevX.7.031041

55. Y. Zhang, Z. He, and P. Li, "Efficient preparation of quantum states for image representation and processing," Quantum Information Processing, vol. 14, pp. 1231–1249, 2015. https://doi.org/10.1007/s11128-015-1049-2

56. J. C. Lee, Y. H. Hwang, and C. Gan, "Quantum digital image processing algorithms based on quantum measurement," Optik, vol. 124, pp. 6386–6390, 2013. https://doi.org/10.1016/j.ijleo.2013.05.063

57. W. Liu, L. Wang, and M. Cui, "Quantum image segmentation based on grayscale morphology," IEEE Transactions on Quantum Engineering, vol. 3, pp. 1–12, 2022. https://doi.org/10.1109/TQE.2022.3223368

58. N. Min-Allah, N. Nagy, M. Aljabri, M. Alkharraa, M. Alqahtani, D. Alghamdi, R. Sabri, and R. Alshaikh, "Quantum image steganography schemes for data hiding: A survey," Applied Sciences, vol. 12, no. 20, art. 10294, 2022. https://doi.org/10.3390/app122010294

59. J. M. Zollner, P. Walther, and M. Werner, "Satellite image representations for quantum classifiers," Datenbank-Spektrum, vol. 24, pp. 33–41, 2024. https://doi.org/10.1007/s13222-024-00464-7

60. M. Parigi, M. Khosrojerdi, F. Caruso, and L. Banchi, "Analysis of quantum image representations for supervised classification," arXiv:2507.22039 [quant-ph], 2025. https://arxiv.org/abs/2507.22039

61. RequieMonk, "Sentinel-1 and Sentinel-2 image pairs segregated by terrain," Kaggle, 2022. [Online]. Available: https://www.kaggle.com/datasets/requiemonk/sentinel12-image-pairs-segregated-by-terrain

62. Tawsifur Rahman, "Tuberculosis (TB) Chest X-ray dataset," Kaggle, 2022. [Online]. Available: https://www.kaggle.com/datasets/tawsifurrahman/tuberculosis-tb-chest-xray-dataset